

POLITECNICO DI TORINO

Master's Degree in Electronic Engineering



Master's Degree Thesis

Project for Antennas for High-Power Electronic countermeasure (ECM) Applications

Supervisors

Chiar.mo Prof. Giuseppe VECCHI

Magg. ing. Daniele FERRANTE

Ing. Giorgio GIORDANENGO

Ing. Marco RIGHERO

Candidate

Ten. ing. Ettore DE MAIO

December 2023

Abstract

The present Master's Thesis project in electronic engineering focuses on the in-depth analysis and precise design of High Frequency (HF) antenna, taking into consideration both ideal and challenging operational conditions. Building upon the CMV-605E antenna as a fundamental reference point, the endeavor entails the creation of a comprehensive Computer-Aided Design (CAD) model for the radiating structure, followed by a rigorous testing phase employing advanced electromagnetic simulation software.

This research holds substantial significance within the military context and is carried out through a collaborative effort between the prestigious LINKS Foundation and Centro Polifunzionale di Sperimentazione (CEPOLISPE), an institute dedicated to research and experimentation within the Italian Army. This collaboration is part of the broader Smart Electronic Protection Measures (SEPROM) project [1], financed by the European Defence Agency, and involves three European nations: Italy, Germany, and Poland .

The ultimate objective of this undertaking is the development of a sophisticated antenna system, purposefully designed for use at CEPOLISPE. The intended application of this antenna is to rigorously assess the performance of various vehicles and electronic devices under conditions characterized by elevated electromagnetic fields (High-Intensity Radiated Fields (HIRF)). This project exemplifies the synergy between cutting-edge technological research and practical applications.

Summary

The present thesis work is based on a close collaboration between the Centro Polifunzionale di Sperimentazione (CEPOLISPE) of the Italian Army and the LINK Foundation, which unfolds through the SEPROM project. This research originates from a need within the European Union to defend one or more member states from potential threats related to Electronic Warfare (EW) attacks. In this context, CEPOLISPE has assumed a leading role with the goal of becoming a reference point in the field of experimentation, both at the national and international levels. The shared objective of both Organizations is the creation of an antenna capable of operating at low frequencies and generating significant electric fields, allowing for the testing of its effects on the functionality of vehicles, devices, and military personnel.

Technological progress and the extensive use of electronic devices based on electromagnetic fields have led to a significant increase in risks, both for human health and the reliability of the devices themselves. Consequently, a deep understanding of the theoretical foundations of electromagnetic fields has become necessary to identify and mitigate potential risks associated with electromagnetic radiation, ensuring the safety of military and civilian personnel.

Furthermore, this knowledge is of great importance in ensuring the safety of munitions, the management and storage of fuel supplies, and the safeguarding of electronic systems used in commerce and operational environments. Therefore, the thesis work has focused on exploring an extremely relevant topic in the field of electromagnetic engineering, considering three fundamental aspects: the theoretical foundations of electromagnetic fields, the impact of high-intensity fields (HIRF), and the known risks such as Hazards of Electromagnetic Radiation to Fuel (HERF), Hazards of Electromagnetic Radiation to Ordnance (HERO), and Hazards of Electromagnetic Radiation to Personnel (HERP).

Before proceeding with the antenna design, it was essential to examine the evolution of wire antennas and their current development. Wire antennas, consisting of simple linear conductors like wires or cables, are common and highly versatile devices in the field of electromagnetic communications. This study provides an in-depth analysis of various types of wire antennas, their operational characteristics, advantages, and limitations. Special attention was given to numerical simulations used to assess their influence on performance and reliability. Innovative technologies and materials that have shown significant potential to enhance the performance of radiating devices were also explored.

Numerical simulations played an essential role in the study of antennas, enabling an accurate evaluation of performance in various scenarios and configurations. In this thesis, the Computer Simulation Technology (CST)-Studio software, widely employed for antenna analysis and design, was used. This software offers a wide range of features for modeling and simulating the electromagnetic behavior of antennas, allowing for a precise assessment of parameters such as radiation, gain, and impedance.

Since the primary requirement was to generate intense electric fields (HIRF), the CMV-600 antenna series [2], specifically the CMV-605E model, was used as a reference point. During the design phase, several preliminary models were developed, with some serving as the basis for the final design, while others were discarded as unsuitable for the project's needs. Optimizing the final design was crucial to maximize antenna efficiency and performance, ensuring the achievement of predefined objectives.

A particularly interesting aspect was observed with the introduction of an obstacle near the radiating element. This was done with the dual purpose of evaluating potential changes in system behaviour, a significant aspect for low-frequency antennas, and assessing the intensity of the electric field impacting the obstacle. However, despite the presence of the obstacle, no significant changes in antenna behaviour were observed, confirming the effectiveness and integrity of the developed design.

Finally, the thesis will conclude by highlighting the challenges faced, summarizing the most important project results, and emphasizing future prospects for research in this field. Understanding the theoretical foundations of electromagnetic fields, exploring the potential of wire antennas through advanced numerical simulations, and developing optimal solutions for High Frequency (HF) antennas represent significant steps in the progress of electronics, with applications spanning from industrial and medical sectors to the military, contributing to the protection of national defense and security.

Acknowledgements

Sono giunto al termine di questo entusiasmante percorso durato due anni, con tanta gioia e consapevolezza nelle mie capacità. Per me questo non è sicuramente un traguardo, ma la rampa di lancio per la mia carriera professionale di Ufficiale dell'Esercito Italiano e di Uomo.

Sembra ieri la prima volta che mettevo piede in questa splendida città, Torino, per dare inizio, con fierezza, con orgoglio e con tanta determinazione agli ultimi due anni di formazione presso la Scuola di Applicazione. Questo antico istituto militare è stato per me una seconda casa, dove ho appreso tutti i valori e le tradizioni "militari" racchiuse al suo interno.

Per questo motivo i primi ringraziamenti voglio porgerli alle Istituzioni dell'Esercito Italiano ed alla Scuola di Applicazione di Torino in quanto sono parte della mia vita e lo saranno per sempre come recita il motto "UNA ACIES". Ringrazio la prestigiosa Università del Politecnico di Torino che, con i suoi esimi Professori, mi ha guidato ed educato in modo ineccepibile fino al conseguimento della Laurea Magistrale.

Un grazie sentito va al Chiar.mo Professore Giuseppe VECCHI, mio Relatore, il quale, con profonda passione e dedizione, mi ha aperto le porte della materia che poi sarà oggetto dei miei impieghi futuri.

Sento il dovere di porgere un ringraziamento anche ai miei Correlatori Magg. ing. Daniele FERRANTE, il dottor Giorgio GIORDANENGO ed il dottor Marco RIGHERO che mi hanno sempre supportato fornendomi un valido aiuto e un grande sostegno.

Prima di ringraziare la mia famiglia e i miei amici, ci tengo a sottolineare la mia gratitudine nei confronti delle Linee di Comando che, con i loro insegnamenti, in questi due anni di Formazione, mi ha reso un uomo disciplinato e rispettoso, capace e in grado di affrontare ogni difficoltà, in un'unica parola un leader.

Ringrazio tutti i miei colleghi del 200° Corso “DOVERE”, in particolare il III Plotone “AENEAS”, i quali sono diventati una seconda famiglia per me dopo tutto quello che abbiamo condiviso e passato insieme.

Un grazie anche a tutti i miei amici con i quali sono cresciuto e quelli che ho conosciuto durante il mio percorso universitario nella città di Torino.

Come anticipato i ringraziamenti più sentiti non possono che essere rivolti alla mia splendida famiglia. Durante questo duro percorso, che mi ha portato lontano da casa, i miei nonni mi hanno sempre appoggiato nella mia scelta insegnandomi, sin da piccolo, quei valori di correttezza, di generosità e di altruismo.

Un ringraziamento speciale alla mia ragazza Mariangela per essere stata sempre al mio fianco con orgoglio e fedeltà. Sei una persona unica che mi ha cambiato la vita dal primo momento che ti ho conosciuta. Hai saputo accettare la mia scelta di diventare un Ufficiale dell'Esercito Italiano, nonostante questo comportasse una vita di sacrifici. Io non posso che esserti riconoscente ed essere fiero di avere una ragazza come te al mio fianco.

Ringrazio la mia splendida sorellina Sara, che mi ha sempre sostenuto nei momenti difficili ed è sempre stata fiera di me e delle mie scelte. Ora che non ci sono più a casa ti sei impossessata della mia camera, ma, nonostante ciò, ti voglio tanto bene.

Il ringraziamento finale, ma non meno importante, va ai miei genitori che per me sono sempre stati una figura di riferimento alla quale ispirarsi. Sin da bambino non mi hanno fatto mancare nulla e mi sono sempre stati vicino nei momenti del bisogno. Per questo e molto altro sono molto riconoscente a loro e a tutti coloro che mi hanno sostenuto ed amato. Dedico la mia Laurea Magistrale in Ingegneria a tutti Voi

Ten. ing. Ettore DE MAIO

Table of Contents

List of Tables	X
List of Figures	XI
Acronyms	XIV
1 Theoretical Foundations	1
1.1 Equations and Parameters	1
1.1.1 The Maxwell's Equations	1
1.1.2 Wave Equations	5
1.1.3 The Green's function	6
1.1.4 Far-field simplifications	7
1.1.5 Power radiated by an elementary dipole	7
1.1.6 Radiation from sources in a finite volume	8
1.1.7 The radiation integral	9
1.2 Electromagnetic Waves	11
1.3 Risks of Electromagnetic Radiation	18
1.3.1 Hazards of Electromagnetic Radiation to Ordnance	18
1.3.2 Hazards of Electromagnetic Radiation to Personnel	20
1.3.3 Hazards of Electromagnetic Radiation to Fuel	23
2 Wire Antennas	26
2.1 State of Art	30
3 Numerical simulations	36
3.1 Software Computer Simulation Technology Studio Suite 2022	36
3.1.1 CST Environment	37
3.2 Electromagnetic modeling	37
3.2.1 The "Finite Integration Technique" Algorithm	37
3.2.2 The Perfect Boundary Approximation (PBA) method	38
3.2.3 The Thin Sheet Technique (TST)	39

3.2.4	The Scattering matrix	39
4	Numerical Results	46
4.1	Design of HF antenna	46
4.1.1	Design phases	49
4.2	Simulation and modeling of HF antenna	54
4.3	Optimization of HF antenna	57
4.3.1	Different design solutions.	57
4.3.2	Reference Impedence optimization	60
4.3.3	Optimizer	61
4.4	Discussion of results and future developments	65
4.4.1	Electric Field Values	65
4.4.2	Simulation with the addition of the military vehicle.	68
5	Conclusions	71
	Bibliography	73

List of Tables

1.1	Maximum external EME levels for ordnance.	19
1.2	ELVs for health effects for internal electric field intensity at frequencies between 1 Hz and 10 MHz.	20
1.3	ELVs for health effects for exposure to electromagnetic fields.	21
1.4	ELV for health effects for exposure to electromagnetic fields.	21
1.5	ELVs for sensory effects for internal electric field at frequencies between 1 Hz and 400 Hz.	22
1.6	ELV for sensory effects for exposure to electromagnetic fields.	22
1.7	AV for contact current (Integrated Circuit (IC))	23

List of Figures

1.1	Elementary electric dipole radiation.	8
1.2	Radiation from a finite volume of sources.	9
1.3	Electromagnetic Waves.	11
1.4	Effect on Flammable Fields due to an Increase in Fuel Temperature.	24
1.5	Temperature-Flammability Regions for Various Common Fuels.	25
2.1	Design of Monopole Antenna made with CST-Studio.	30
2.2	Design of Marconi Antenna made with CST-Studio.	31
2.3	Design of Wire Dipole Antenna made with CST-Studio.	32
2.4	Design of Folded Dipole Antenna made with CST-Studio.	33
2.5	Yagi-Uda antenna.	35
3.1	Two-port device with the definitions of voltage and current at the ports.	40
4.1	Antenna from the CMV-600 series.	47
4.2	Design of an umbrella antenna.	48
4.3	Initial working window.	49
4.4	Creation of the ground plane.	50
4.5	Creation of the vertical element.	50
4.6	Translation of the hexagonal base of the cone.	51
4.7	Creation of the internal reinforcing structure.	52
4.8	Creation of the connecting wires for the conical structure.	52
4.9	Final design of the antenna.	53
4.10	Discrete port.	53
4.11	Parameter list.	54
4.12	Aluminum data sheet.	55
4.13	PEC data sheet.	56
4.14	First variant: open cone configuration.	57
4.15	Second variant: cone tip configuration with internal structure.	58
4.16	S-Parameters plot comparison.	58

4.17	Par. Sweep of Reference Impedence	60
4.18	S-parameters of the antenna with optimization of the Reference Impedence	61
4.19	Optimizer.	62
4.20	New parameter list.	64
4.21	E-Field ($f = 30$ MHz)	65
4.22	Rescaling of the E-Field ($f = 22.5$ MHz) with $X = 0.35$ m	66
4.23	Rescaling of the E-Field ($f = 22.5$ MHz) with $X = 1.55$ m	66
4.24	Rescaling of the E-Field ($f = 22.5$ MHz) with $X = 4.60$ m	67
4.25	Final design with the presence of the vehicle.	68
4.26	Comparison between the ideal simulation and the simulation with the presence of the medium.	69
4.27	Sub-volume Simulation	69
4.28	Simulation of the sub-volume.	70
4.29	Frontal view simulation of the sub-volume.	70

Acronyms

AV

Action Values

CAD

Computer-Aided Design

CST

Computer Simulation Technology

CEPOLISPE

Centro Polifunzionale di Sperimentazione

ECM

Electronic countermeasure

EID

Explosive Initiation Devices

ELV

Exposure Limit Values

EMC

Electromagnetic compatibility

EME

Electromagnetic Environment

EMR

Electromagnetic radiation

EW

Electronic Warfare

FIT

Finite Integration Technique

gnd

ground

HERF

Hazards of Electromagnetic Radiation to Fuel

HERO

Hazards of Electromagnetic Radiation to Ordnance

HERP

Hazards of Electromagnetic Radiation to Personnel

HF

high-frequency

HIRF

High-Intensity Radiated Fields

IC

Integrated Circuit

ICNIRP

International Commission on Non-Ionizing Radiation Protection

IR

Ionizing Radiation

MNFS

Minimum Non-Firing Stimulus

MOGAS

Motor Gasoline

NIR

Non-Ionizing Radiation

PBA

Perfect Boundary Approximation

PEC

Perfect Electric Conductor

RF

Radio Frequency

SEPROM

Smart Electronic Protection Measures

SAR

Specific Absorption Rate

SUT

System Under Test

TST

Thin Sheet Technique

VLF

Very Low Frequency

WHO

World Health Organization

Chapter 1

Theoretical Foundations

1.1 Equations and Parameters

1.1.1 The Maxwell's Equations

All the electromagnetic phenomena are described by the Maxwell's Equations [3], represented by a system of partial derivative equations.

$$\begin{cases} \nabla \times \underline{E}(\underline{r}, t) = -\frac{\partial}{\partial t} \underline{B}(\underline{r}, t) \\ \nabla \times \underline{H}(\underline{r}, t) = \frac{\partial}{\partial t} \underline{D}(\underline{r}, t) + \underline{J}_e(\underline{r}, t) \end{cases} \quad (1.1)$$

Where:

- $\underline{E}(\underline{r}, t)$: ELECTRIC FIELD, measured in [V/m];
- $\underline{B}(\underline{r}, t)$: MAGNETIC INDUCTION, measured in [Wb/m²];
- $\underline{H}(\underline{r}, t)$: MAGNETIC FIELD, measured in [A/m];
- $\underline{D}(\underline{r}, t)$: ELECTRIC DISPLACEMENT, measured in [As/m²];
- $\underline{J}_e(\underline{r}, t)$: ELECTRIC CURRENT DENSITY, measured in [A/m²].

Among these terms, the electric current density can be of different types:

- J_i : IMPRESSED CURRENT The impressed current is the current provided from the external current source.

In turn, this current can be of two different types:

1. J_c : CONDUCTION CURRENT This current is the one that flows in elements having free moving charges. It is present in materials that have a conductivity different from zero, where electrons are free to move due to the application of an electric field.

The conduction current is typically governed by Ohm's law, which relates the current to the electric field and the conductivity of the material.

In general, the conduction current density J_c can be expressed as:

$$J_c = \sigma \cdot E \quad (1.2)$$

where:

- J_c is the conduction current density;
- σ is the electrical conductivity of the material;
- E is the electric field.

This equation states that the conduction current density is directly proportional to the electrical conductivity and the electric field. The direction of the conduction current is typically aligned with the direction of the electric field.

2. J_d : DISPLACEMENT CURRENT This current originates from the displacement of bound charges within the atom and manifests as an apparent current induced by the time-varying electric field.
- J_p : PLASMA CURRENT The plasma current refers to the flow of electric current carried by charged particles within a plasma.

Returning to Maxwell's equations, the system starts with two first-order differential equations. To simplify their form, the approach involves separating the spatial derivative from the temporal derivative. To illustrate this concept, a generic phasor \underline{A} is considered, which depends on both the three spatial variables and time.

$$\underline{A}(r, t) = \Re \left\{ \underbrace{\underline{A}(r)}_{\text{SPACE}} \cdot \overbrace{e^{j\omega_0 t}}^{\text{TIME}} \right\} \quad (1.3)$$

while the time derivative of \underline{A} is:

$$\frac{\partial}{\partial t} \underline{A}(r, t) = \frac{\partial}{\partial t} \Re \underline{A}(r) e^{j\omega_0 t} \quad (1.4)$$

In conclusion, after a series of mathematical steps, the time derivative of a phasor is the phasor itself times $j\omega_0$. Therefore, in the initial system, we can make the following substitution:

$$\frac{\partial}{\partial t} \rightarrow j\omega_0$$

As a result, the system (1.1) becomes:

$$\begin{cases} \nabla \times \underline{E}(\underline{r}) = -j\omega_0 \underline{B}(\underline{r}) \\ \nabla \times \underline{H}(\underline{r}) = j\omega_0 \underline{D}(\underline{r}) + \underline{J}_e(\underline{r}) \end{cases} \quad (1.5)$$

To further simplify the previous system, we can apply the divergence operator $\nabla \cdot$ to each equation, yielding:

$$\begin{cases} \underbrace{\nabla \cdot (\nabla \times \underline{E}(\underline{r}))}_{\equiv 0} = -j\omega_0 \nabla \cdot \underline{B}(\underline{r}) \\ \underbrace{\nabla \cdot (\nabla \times \underline{H}(\underline{r}))}_{\equiv 0} = j\omega_0 \nabla \cdot \underline{D}(\underline{r}) + \nabla \cdot \underline{J}_e(\underline{r}) \end{cases} \quad (1.6)$$

In the end the two terms, highlighted in the previous system, are equal to zero, so:

$$\begin{cases} 0 = -j\omega_0 \nabla \cdot \underline{B}(\underline{r}) \\ 0 = j\omega_0 \nabla \cdot \underline{D}(\underline{r}) + \nabla \cdot \underline{J}_e(\underline{r}) \end{cases} \quad (1.7)$$

Based on these results, we can draw some conclusions:

- The magnetic induction B remains constant.
- There exists an inherent system asymmetry, as evidenced by the inclusion of the electric current density J_e in the second equation while its absence in the first equation. This asymmetry arises from the absence of magnetic charges in nature, which precludes objects from experiencing motion solely induced by a magnetic field.
- A relationship can be established between the electric current density J_e and the charge density ρ . Applying a potential difference to a specified set of charges within a volume triggers their motion, causing a decrease in charge density and an increase in current.

Then the Maxwell's Equations describe the movement of charges in a medium:

$$\begin{cases} \nabla \cdot \underline{B}(\underline{r}) = 0 \\ \nabla \cdot \underline{D}(\underline{r}) = \rho(\underline{r}) \end{cases} \quad (1.8)$$

Inside $\underline{\mathbf{B}}$ and $\underline{\mathbf{D}}$, which are related to the magnetic field and the electric field respectively, the electric permittivity ϵ and the magnetic permeability μ can be found.

Therefore, in the case of a medium that is homogeneous, isotropic, and linear, the permittivity and permeability are no longer tensors but are constants, specifically:

$$\epsilon = \epsilon_r \epsilon_0 \tag{1.9}$$

$$\mu = \mu_r \mu_0 \tag{1.10}$$

However, to simplify further, $\mu_r \approx 1$, so:

$$\mu = \mu_0$$

In the end, the homogeneous system is obtained in the absence of an external source ($J_e = 0$), so:

$$\begin{cases} \nabla \times \underline{\mathbf{E}}(\underline{\mathbf{r}}) = -j\omega_0 \mu \underline{\mathbf{H}}(\underline{\mathbf{r}}) \\ \nabla \times \underline{\mathbf{H}}(\underline{\mathbf{r}}) = j\omega_0 \epsilon \underline{\mathbf{E}}(\underline{\mathbf{r}}) \end{cases} \tag{1.11}$$

1.1.2 Wave Equations

The wave equations [3][4] are mathematical equations that describe the behaviour and propagation of waves. The wave equation represents how the wave's amplitude, frequency, and wavelength change over time and space.

In this case is applied the curl operator $\nabla \times$, so:

$$\begin{cases} \nabla \times (\nabla \times \underline{E}(\underline{r})) = -j\omega_0\mu (\nabla \times \underline{H}(\underline{r})) \\ \nabla \times (\nabla \times \underline{H}(\underline{r})) = j\omega_0\epsilon(\nabla \times \underline{E}(\underline{r})) \end{cases} \quad (1.12)$$

Referring to the theory, it is recalled that when considering a generic vector \underline{A} , the curl operation returns another vector, denoted as \underline{B} . Therefore, when applying the curl operation once again to vector \underline{B} , a vector is obtained as well.

In this case, after a series of simplifications, wave equations or Helmholtz equations are derived.

$$\begin{cases} \nabla^2 \underline{E}(\underline{r}) + \tilde{k}^2 \underline{E}(\underline{r}) = 0 \\ \nabla^2 \underline{H}(\underline{r}) + \tilde{k}^2 \underline{H}(\underline{r}) = 0 \end{cases} \quad (1.13)$$

In other words, when J_e is not equal to zero, it indicates the presence of losses, and the electric permittivity is not solely determined by $\epsilon = \epsilon_r \epsilon_0$. Instead, the quantity $\tilde{\epsilon}$ needs to be considered.

Thanks to a simplification, the term $\sigma = \omega_0\epsilon$ is referred to as the dielectric loss tangent $\tan \delta$, which is a dispersing quantity dependent on the angular frequency. Based on the value of \tilde{k} , two distinct scenarios will emerge:

- If the system is lossless:

$$\tilde{k} = k = \omega \sqrt{\epsilon\mu}$$

- If the system is with losses:

$$\tilde{k} = \omega \sqrt{\tilde{\epsilon}\mu} = k_0 \sqrt{\epsilon_r \mu_r}$$

Therefore, in far-field conditions, the solution of the Helmholtz equation becomes:

$$\underline{E}(\underline{r}) = \underline{E}_0 e^{\pm jkr} \quad (1.14)$$

1.1.3 The Green's function

The Green's function [3] facilitates the expression of the solution to a linear differential equation as a superposition of solutions to simpler problems.

Considering again the Maxwell's Equation:

$$\begin{cases} \nabla \times \underline{E}(\underline{r}) = -j\omega_0\mu \underline{H}(\underline{r}) + \underline{J}_m(\underline{r}) \\ \nabla \times \underline{H}(\underline{r}) = j\omega_0\epsilon \underline{E}(\underline{r}) + \underline{J}_e(\underline{r}) \end{cases} \quad (1.15)$$

The electric field $\underline{E}(\underline{r})$ and the magnetic field $\underline{H}(\underline{r})$ are the unknowns, while $\underline{J}_e(\underline{r})$ and $\underline{J}_m(\underline{r})$ are known terms acting as sources for the electromagnetic fields.

The idea is to start from the sources and, applying a transfer function, obtain the expressions of $\underline{E}(\underline{r})$ and $\underline{H}(\underline{r})$.

$$\begin{bmatrix} \underline{J}_e(\underline{r}) \\ \underline{J}_m(\underline{r}) \end{bmatrix} \rightarrow \boxed{\text{TRANSFER FUNCTION}} \rightarrow \begin{bmatrix} \underline{E}(\underline{r}) \\ \underline{H}(\underline{r}) \end{bmatrix}$$

The link between the current densities and the fields is the dyadic Green's function $\underline{\underline{G}}$ and the final solution of the electric field is the following one:

$$\underline{E}(\underline{r}) = -j\omega\mu \int_{r'} \underline{\underline{G}}(\underline{r}, \underline{r}') \cdot \underline{J}_e(\underline{r}') d\underline{r}' + j \int_{r'} \nabla \times \underline{\underline{G}}(\underline{r}, \underline{r}') \cdot \underline{J}_m(\underline{r}') d\underline{r}' \quad (1.16)$$

where the explicit expression of the dyadic Green's function is:

$$\underline{\underline{G}} = \left[\hat{r}\hat{r} \left(\frac{2j}{k_0r} + \frac{2}{(k_0r)^2} \right) + \hat{\theta}\hat{\theta} \left(1 - \frac{j}{k_0r} - \frac{1}{(k_0r)^2} \right) + \hat{\varphi}\hat{\varphi} \left(1 - \frac{j}{k_0r} - \frac{1}{(k_0r)^2} \right) \right] \Phi \quad (1.17)$$

The term Φ is called scalar Green's function and it is given by the following expression:

$$\Phi = \frac{e^{-jkr}}{4\pi r}$$

Examining the expression of the electric field given in the previous equation, it is evident that there is consistently a component parallel to the electric current density \underline{J}_e . On the other hand, the contribution arising from the magnetic current density \underline{J}_m is orthogonal as a result of applying the curl operator $\nabla \times$.

1.1.4 Far-field simplifications

In the far-field region [4], where the observation point is significantly distant from the origin, it becomes possible to simplify the dyadic Green's function, which is dependent on the distance, r . In this regime, as r tends to infinity, it follows that kr also tends to infinity. Consequently, the terms $1/k_0r$ and $1/(k_0r)^2$ can be neglected since they approach zero.

Therefore, when considering the Green's function in the far-field, the following simplifications can be made:

$$\underline{\underline{G}} \cong (\hat{\theta}\hat{\theta} + \hat{\varphi}\hat{\varphi}) \Phi \quad (1.18)$$

1.1.5 Power radiated by an elementary dipole

In the typical scenario [4], there is a transmitting antenna (TX) that generates a power density, and a receiving antenna (RX) that ideally captures this power density, assuming negligible losses.

The objective is to determine the total power radiated by the transmitting antenna, which is currently modelled as an elementary electric dipole. To accomplish this, the starting point is the Poynting vector $\underline{S}(\underline{r})$, which represents the power density associated with the radiation of the elementary dipole at each point in space.

By integrating the power density over a closed sphere, the total power within the designated surface can be obtained.

For definition, the Poynting vector can be computed as:

$$\underline{S}(\underline{r}) = \underline{E}(\underline{r}) \times \underline{H}(\underline{r})^* \quad (1.19)$$

In this case, the electric field presents a component along the r -direction and a component along the θ -direction, while the magnetic field has only one component along the φ -direction.

After a series of steps and mathematical simplifications, along the θ -direction, there is no active power flux.

For the elementary electric dipole placed at the origin of our system, we have that S_θ is all concentrated near the source, so around the origin, we have a concentration of reactive energy (because S_θ is completely imaginary) that decays very fast far from the origin. In conclusion, the total power radiated is given by:

$$P = \int_{\Sigma} \frac{Z_0 M^2}{4r^2 \lambda^2} \sin^2 \theta d\Sigma$$

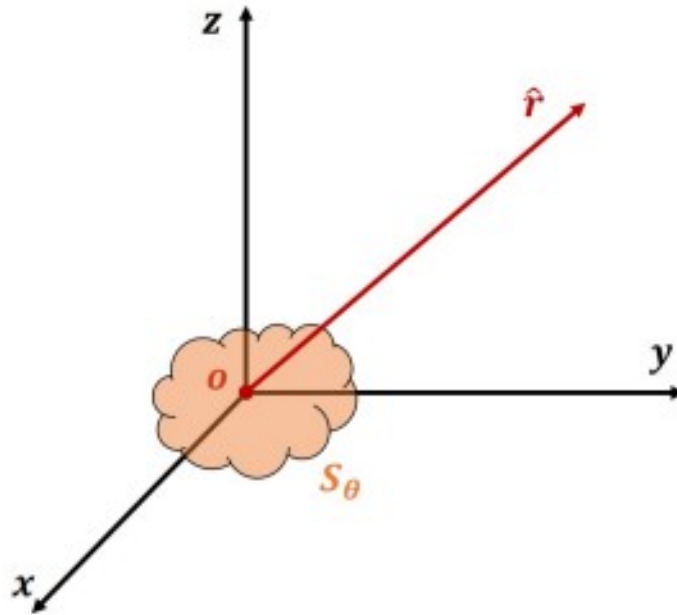


Figure 1.1: Elementary electric dipole radiation.

In the context of a lossless scenario, the derived result indicates that the power radiated by the transmitting antenna remains constant regardless of the distance. This observation aligns with the fundamental principle of energy conservation.

1.1.6 Radiation from sources in a finite volume

To investigate the repercussions of multiple radiation sources, one must consider a finite volume that encompasses electric and magnetic sources with distinct orientations. The observation point P is located outside the volume, while a reference point O is positioned within it. This setup facilitates the examination of the consequences that arise when dealing with non-elementary sources.

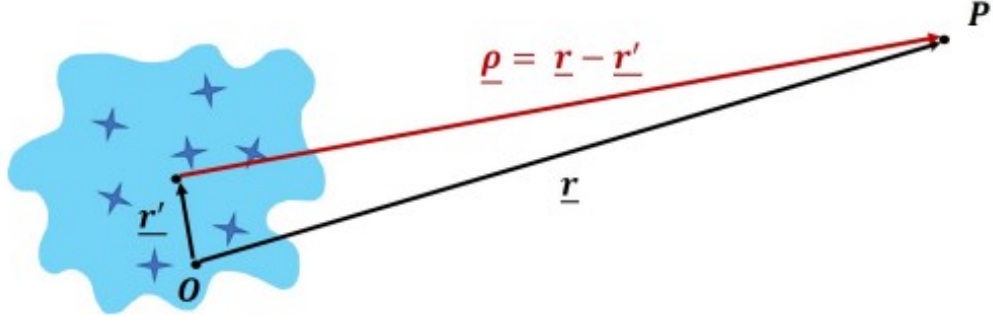


Figure 1.2: Radiation from a finite volume of sources.

The formula consists of the following parameters:

- \underline{r} is the position vector from the origin O to the observation point P .
- \underline{r}' is the vector from the origin O to the sources.
- $\underline{\rho}$ is the difference between the two vectors.

By definition, if we have two vectors, the distance between them can be calculated as the norm of their difference. In our case, it can be calculated as the norm of ρ . The square of the norm of the vector ρ is evaluated in the following way:

$$||\rho||^2 = r^2 - 2r\hat{r} \cdot \hat{r}' + r'^2 \quad (1.20)$$

Performing arithmetic calculations and using Taylor's approximation, it is obtained that the error on Ψ , denoted as $\Delta\Psi$, is proportional to the error on $\Delta\rho$. Mathematically, this can be expressed as:

$$\Delta\Psi = k\Delta\rho = k\frac{1}{2r} [r'^2 - (\underline{r}' \cdot \hat{r})^2] \quad (1.21)$$

This implies that if there is an increase in the error on $\Delta\rho$, the error on Ψ will also increase, and vice versa. The proportionality relationship allows for the estimation of the impact of the error on $\Delta\rho$ on the resulting error in Ψ .

1.1.7 The radiation integral

It serves as a mathematical tool to determine the electromagnetic field at any given point in space resulting from the distribution of sources within the volume.

Mathematically, the radiation integral [3] can be expressed as:

$$\varphi(\underline{r}) = \int \int \int \underline{G}(\underline{r}, \underline{r}') \cdot \underline{\rho}(\underline{r}') dV' \quad (1.22)$$

where:

- $\varphi(\underline{r})$ represents the radiated field at a point \underline{r} in space.

- $\underline{\underline{G}}(\underline{r}, \underline{r}')$ denotes the Green's function, which characterizes the system's response to a point source located at \underline{r}' .

- $\underline{\rho}(\underline{r}')$ represents the source distribution within the volume, typically expressed as a charge or current density.

- dV' denotes an infinitesimal volume element within the source distribution.

The radiation integral effectively integrates the contributions from all source elements within the volume, taking into account their spatial distribution and mutual interaction. The Green's function accounts for the propagation and interaction of electromagnetic waves within the system, incorporating the geometry and boundary conditions associated with the finite volume.

Solving the radiation integral involves evaluating the Green's function and performing the integration over the volume occupied by the sources. Analytical solutions may not always be feasible, depending on the complexity of the system and the characteristics of the sources. In such cases, numerical methods, such as numerical integration or discretization techniques, are employed to approximate the integral and compute the radiated field.

1.2 Electromagnetic Waves

Electromagnetic waves [5] are a physical phenomenon through which electromagnetic energy can transfer from one place to another using the principle of "propagation." This energy transfer can occur in free space without the need for any other systems, or it can be confined and facilitated using appropriate transmission lines (waveguides, coaxial cables, etc.).

According to Maxwell's theory, electromagnetic waves are oscillatory phenomena, generally of a sinusoidal nature, and they are composed of two quantities that vary periodically over time: the electric field and the magnetic field.

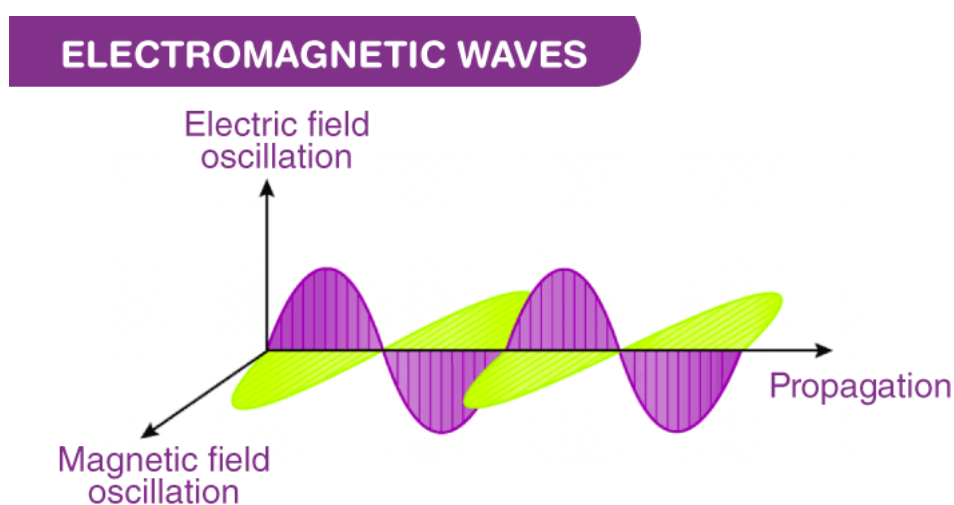


Figure 1.3: Electromagnetic Waves.

The electric field E [6] is defined as a characteristic or perturbation of space produced by the presence of electric charges, either positive or negative. This perturbation can be experimentally observed by detecting the presence of a force when placing an electric charge in the perturbed region. Any electric conductor produces an associated electric field, which exists even when no current flows through the conductor. The intensity of the electric field is measured in volts per meter (V/m). The higher the voltage, the stronger the field generated by it, and the greater the distance from the conductor at which it can be detected. For a given voltage, the intensity of the field decreases as the distance from the conductor increases.

On the other hand, the magnetic field H can be defined as a property or perturbation of space produced by the movement of electric charges within it, the presence of electric currents, or permanent magnets.

Once again, this perturbation can be experimentally detected by placing a magnetized object in the perturbed region, which experiences a force. The intensity of the magnetic field is expressed in amperes per meter (A/m), although it is common to refer to a related quantity, the magnetic flux density or magnetic induction B , measured in microteslas (μT). It is important to remember that the following relationship holds between the two units of measurement: $1 \text{ T} = 7.958 \times 10^5 \text{ A/m}$, and the magnetic field is generated only when an electrical appliance is turned on and there is a current flow. Its intensity is directly proportional to the magnitude of the electric current. Magnetic fields are more intense in proximity to the source and rapidly decrease as the distance from it increases. Additionally, unlike electric fields, they are not shielded by common materials, such as building walls.

A time-varying electric field generates, perpendicular to itself, a time-varying magnetic field, which in turn influences the electric field. These interrelated fields give rise to the propagation of an electromagnetic field in space, independent of the electric charges and currents that generated them. In the vicinity of the radiating source, that is, under conditions of very close fields, the electric field and the magnetic field assume varying ratios depending on the distance and can be considered separately. However, at a greater distance, under conditions of far fields, the ratio between the electric field and the magnetic field remains constant: in far field conditions, the two fields are in phase, on orthogonal planes to each other and transverse to the direction of propagation (plane electromagnetic wave).

The main characteristics of electromagnetic waves depend on one fundamental property: frequency f , which is the number of oscillations completed in one second. This quantity is measured in cycles per second or hertz (Hz) and its related multiples and submultiples [7].

Closely related to frequency is the wavelength λ , which is defined as the distance traveled by the wave during one oscillation period and corresponds to the distance between two wave maxima or minima (the unit of measurement is the meter with its multiples and submultiples). The two quantities are inversely proportional to each other through the following relationship:

$$f = \frac{v}{\lambda}$$

where v is the propagation velocity of the wave, expressed in meters per second (m/s).

It is important to remember that these waves also propagate in a vacuum, where their propagation velocity is 300,000 km/s.

These two quantities, frequency and wavelength, are not only related to each other but also connected to the energy E carried by the wave, which, in turn, has two different units of measurement: the joule (J) and its multiples or the electronvolt (eV). The conversion relationship between these two units of measurement is: $1 \text{ J} = 6.24 \times 10^{18} \text{ eV}$.

This energy associated with electromagnetic radiation is directly proportional to the frequency of the wave itself through the relationship:

$$E = h \cdot f$$

where h is a constant known as the Planck constant, equal to $6.626 \times 10^{-34} \text{ Js}$.

The electromagnetic energy carried by the wave per unit time and unit area is defined as power density S and is expressed in watts per square meter (W/m^2). The higher the frequency value, the greater the amount of energy carried by the wave. When an electromagnetic wave encounters an obstacle, it penetrates into the material and releases a portion of its energy, producing a series of different effects depending on its frequency.

The mechanisms of interaction between radiation and matter determine the effects and potential risks to human health. The set of all possible electromagnetic waves, based on their frequency and different wavelengths, constitutes the Electromagnetic Spectrum.

Within the Electromagnetic Spectrum, two main regions can be distinguished:

- The region where Ionizing Radiation (IR) can be found, when electromagnetic waves have the following characteristics:
 - Frequency higher than 3000 THz.
 - Wavelength shorter than 100 nm.
 - Energy greater than 12.4 eV, which is necessary to break the chemical bonds holding atoms and molecules together and therefore ionize matter.
- The region of Non-Ionizing Radiation (NIR), when electromagnetic waves have a lower frequency and do not carry enough energy to break chemical bonds and cause ionization. It is in this region of the electromagnetic spectrum that we specifically refer to Electromagnetic Fields.

Among the numerous types and characteristics of Electromagnetic Fields, this work will exclusively address and analyze High-Intensity Electromagnetic Fields, which belong to the category of High-Power Electromagnetic Fields generated by external sources such as radar, wireless communications, and electrostatic discharges.

The study focuses on HIRF [8] due to their advantages in various sectors, such as the military field, where high-intensity fields are used for numerous applications, including:

- **Military communications**: In this sector, HIRF is essential for military communications as it enables the transmission of critical data (order packets to combat units, artillery intervention orders, etc.) between units deployed on the battlefield and different command levels stationed in various operational areas. Military communication systems, such as High-Frequency (HF) radios, microwave radios, and satellites, use HIRF to ensure the security and reliability of communications, including the use of encrypted/cryptographic systems. For example, transmissions utilize high-frequency radio waves that can cover long distances and overcome natural or artificial obstacles typically present on the battlefield.
- **Radar system implementation**: Military radars utilize HIRF to detect, track, and identify objects in the sky, on land, or at sea. These surveillance systems are crucial for air defense and target localization on the battlefield based on their nature. HIRF generated by radars reaches high power levels and requires significant protection measures to avoid interference with other electronic systems and the radars themselves.
- **Electronic warfare**: EW encompasses activities aimed at disrupting, deceiving, or neutralizing adversary capabilities that rely on electronic systems. HIRF is used as a means to disturb or disable the electronic systems used by the adversary, including communications, radars, and missile guidance systems, among others. These disruptive actions can be achieved through the emission of jamming signals that interfere with the adversary's sensors, masking one's own tracks or deceiving their detection systems.
- **Electronic countermeasures**: ECM are measures taken to elude or reduce the effectiveness of enemy electronic threats. HIRF is utilized as part of ECM to generate jamming signals that interfere with their sensors. This can confuse detection systems, making it difficult for the adversary to obtain accurate and precise information about the position, velocity, magnitude, and posture of opposing forces, denying them the time to organize a potential offensive action.

- **Development of imaging using advanced sensors:** HIRF also finds applications in image processing and the collection of a large amount of data derived from the use of advanced sensors employed in defense. High-intensity infrared sensors and high-resolution imaging systems, for example, utilize HIRF to generate detailed battlefield images, monitor enemy activities, and acquire tactical information for planning and conducting offensive and defensive coalition operations. Analyzing and examining this data can be crucial for the Operation Commander, who must make important decisions on which course of action to take to fulfill their mission in a very short time.
- **Scientific research:** Finally, HIRF plays a crucial role in studying material properties and particle physics. They can be employed in experiments related to nuclear fusion and the research and efficiency of clean energy sources. Moreover, HIRF is essential in the aerospace sector as they are used in communication, navigation, and flight control systems of aircraft and spacecraft.

However, HIRF also poses some risks. Electromagnetic interference caused by HIRF can negatively affect electronic systems, causing malfunctions, communication errors, or even hazardous situations for living organisms. Therefore, it is necessary to implement HIRF mitigation measures in compliance with electromagnetic compatibility regulations and standards to ensure that electronic devices and systems are designed, produced, and used safely and reliably.

International organizations such as the World Health Organization (WHO), the International Commission on Non-Ionizing Radiation Protection (ICNIRP) [9], and d.lgs. 159-2016 [10] prescribe guidelines and exposure limits based on available scientific evidence from research studies. These limits aim to ensure that HIRF exposure remains below a certain safety threshold for the entire civilian population, with higher limits for vulnerable individuals.

Electronic devices, on the other hand, are susceptible to the effects of HIRF because their components can act as antennas, capturing and transferring energy from electromagnetic fields. HIRF can induce voltages, currents, and electrical interference in circuits, compromising the performance and safety of their systems.

It is evident, therefore, that protection against HIRF is essential to ensure the reliability and performance of electronic devices and, importantly, the safety of people who use these devices or are in their vicinity. This aspect is addressed during the design phase of HIRF by employing mitigation measures that reduce the harmful effects on individuals.

One of the most commonly used techniques for this purpose is electromagnetic shielding, which involves the use of conductive materials to create a protective shell around HIRF-sensitive electronic components. This shielding shell reduces the impact of HIRF on electronic devices, preventing electromagnetic waves from damaging the circuits themselves.

Another method commonly used is based on the use of specific types of filters capable of reducing the signal power. Filters are electronic devices that attenuate unwanted frequencies of high-intensity fields, allowing only a specific frequency band to pass through. This reduces interference and protects sensitive circuits from harmful electromagnetic waves. Grounding systems, when properly developed, are essential for ensuring safety and protection. Grounding allows unwanted currents produced by HIRF to be diverted to the ground, reducing potential damage to electronic devices. Furthermore, grounding also helps prevent the propagation of electrical interference among different components of a system.

Additionally, a valid criterion used during the design and construction of electronic circuits is to isolate sensitive circuits by separating them from devices that emit electromagnetic waves. This is typically achieved using electromagnetic screens or physical barriers to create separation between the various circuits that make up the device. In fact, the large-scale design of electronic devices takes HIRF into account from the early stages of development. It is based on the adoption of specific guidelines that adhere to construction standards satisfying particular requirements to ensure that electronic components are designed and constructed to withstand the effects of HIRF. Material selection, component arrangement, and circuit layout optimization are important considerations in designing equipment that effectively resists HIRF.

The resistance of various circuits is verified through empirical tests that evaluate the effectiveness of the implemented mitigation measures. Through tests such as Electromagnetic compatibility (EMC) tests, it is possible to verify if electronic devices meet the standards and regulations regarding HIRF. Furthermore, these tests identify any issues or vulnerabilities, enabling necessary corrections to be made during the design and construction phase.

Another crucial aspect is the education and training of operators to ensure proper HIRF management. Operators need to be aware of the risks associated with HIRF and the mitigation measures to be adopted. Adequate training should include an understanding of the principles underlying electromagnetic waves, the correct use of electronic equipment, and safety procedures to reduce the exposure of personnel to HIRF.

In summary, HIRF refers to high-power electromagnetic fields generated by external sources that, although they can cause interference and problems in electronic devices, also offer significant advantages in military applications, communications, medicine, scientific research, and the aerospace industry. Protection and mitigation of HIRF are essential to ensure the safety of living organisms, the reliability and performance of electronic systems, which, thanks to technological advancements, have become commonly used in society.

1.3 Risks of Electromagnetic Radiation

The main risks associated with electromagnetic radiation can be classified into three types:

1. Electromagnetic Radiation to Ordnance (HERO)
2. Hazards of Electromagnetic Radiation to Personnel (HERP)
3. Hazards of Electromagnetic Radiation to Fuel (HERF)

These risks encompass a range of potential electromagnetic threats that can have significant effects on electronic systems, with consequences for ordnance, personnel, and fuel. They are associated with phenomena such as hazards of electromagnetic radiation to ordnance (HERO), hazards of electromagnetic radiation to personnel (HERP), and hazards of electromagnetic radiation to fuel (HERF) [11][12].

1.3.1 Hazards of Electromagnetic Radiation to Ordnance

The **HERO** refers to risks associated with electromagnetic radiation to ammunition and explosive devices. Electromagnetic explosions can generate intense electromagnetic fields that can affect the electronic systems within the ammunition or devices. Safety devices such as electronic fuses, ignition circuits, or detonators can be sensitive to electromagnetic radiation. Interaction with the electromagnetic pulse can result in premature activation of ammunition, accidental ignition, or malfunctioning of safety systems, posing risks to military or civilian personnel and causing significant material damage.

Ammunition containing Explosive Initiation Devices (EID) must remain safe and operational during and after exposure to external levels of Electromagnetic Environment (EME) indicated in Table 1.1, both for Radio Frequency (RF) induced direct activation of Explosive Initiation Devices (EID) and accidental activation of an electrically powered ignition circuit. In order to be classified as "HERO SAFE MUNITIONS" at the complete assembly or appropriate assembly level, the ammunition or System Under Test (SUT) must be evaluated against Table 1 and comply with it. Compliance should be verified through testing, analysis, or a combination of both. EIDs must have a Minimum Non-Firing Stimulus (MNFS) threshold of at least 16.5 dB for safety and 6 dB for other applications.

Table 1.1: Maximum external EME levels for ordnance.

Frequency Range MHz		Field Intensity (V/m – rms)			
		Unrestricted ¹		Restricted ²	
		Peak	Average	Peak	Average
0.01	2	200	200	80	80
2	30	200	200	100	100
30	150	200	200	80	80
150	225	200	200	70	70
225	400	200	200	100	100
400	700	2200	410	450	100
700	790	700	190	270	270
790	1000	2700	490	1400	270
1000	2000	6100	420	2500	160
2000	2700	6000	500	490	160
2700	3600	27460	5350	2500	220
3600	4000	8600	280	1900	200
4000	5400	9200	660	650	200
5400	5900	9200	660	6200	240
5900	6000	9200	640	550	240
6000	7900	3190	670	3190	240
7900	8000	2500	670	550	200
8000	8400	7500	450	1100	200
8400	8500	7500	400	1100	200
8500	11000	7500	3450	2000	300
11000	14000	7500	650	3500	220
14000	18000	7900	660	7900	250
18000	50000	2900	580	2800	200

¹It must be noted that on some platforms, there are radar systems that may produce fields in excess of those in Table 1.1, and MIL-HDBK-235 [11] must be consulted to identify specific EME.

²In some of the frequency ranges for the “Restricted Average” column, limiting the exposure of personnel through time averaging will be required to meet the requirements for personnel safety.

1.3.2 Hazards of Electromagnetic Radiation to Personnel

The **HERP** refers to risks associated with time-varying electromagnetic radiation up to frequencies of 300 GHz to military and civilian personnel. Studies conducted so far have identified various potential effects. **Direct biophysical effects:** Effects directly caused in the human body due to its presence within an electromagnetic field, including:

1. **Thermal effect**, which represent one of the main mechanisms through which EMR can influence human health, such as tissue heating due to the absorption of energy from electromagnetic fields in the tissues themselves. In this case, specific safety considerations are given by *ELV for Health Effects* and *AV*. These values are established based on biophysical and biological considerations, particularly based on scientifically established acute and short-term direct effects. Consequently, above these ELVs, workers may be subject to harmful health effects such as thermal heating or stimulation of nervous or muscular tissue.

Table 1.2: ELVs for health effects for internal electric field intensity at frequencies between 1 Hz and 10 MHz.

Frequency Range	ELV for Health Effects [Vm^{-1}] (peak value)
$1 \text{ Hz} \leq f < 3 \text{ kHz}$	1.1
$3 \text{ kHz} \leq f \leq 10 \text{ MHz}$	$3.8 \times 10^{-4} f$

Table 1.3: ELVs for health effects for exposure to electromagnetic fields.

ELV for Health effects	Average SAR values over each six-minute period [Wkg ⁻¹]
ELV for systemic thermal stress, expressed as whole-body average SAR	0.4
ELV for localized thermal stress in the head and torso, expressed as local SAR (in the head and torso)	10
ELV for localized thermal stress in the limbs, expressed as local SAR (in the limbs)	20

Table 1.4: ELV for health effects for exposure to electromagnetic fields.

Frequency Range	Power Density (Wm ⁻²)
6 GHz ≤ f ≤ 300 GHz	50

2. Non-thermal effects, which encompass biological effects not related to increased temperature, such as the stimulation of muscles, nerves, and sensory organs. These effects can be detrimental to the mental and physical health of exposed workers. Furthermore, stimulation of sensory organs can lead to transient symptoms such as dizziness and phosphenes. These effects can generate temporary disturbances and impact cognitive abilities or other brain or muscular functions, thus negatively affecting a worker's ability to operate safely. Similar to thermal effects, safety is regulated by *ELVs for Sensory Effects* and AV.

Table 1.5: ELVs for sensory effects for internal electric field at frequencies between 1 Hz and 400 Hz.

Frequency Range	ELV for Health Effects [Vm^{-1}] (peak value)
$1 \text{ Hz} \leq f < 10 \text{ Hz}$	$0.7/f$
$10 \text{ Hz} \leq f \leq 25 \text{ Hz}$	0.7
$25 \text{ Hz} \leq f \leq 400 \text{ Hz}$	$0.0028 f$

Table 1.6: ELV for sensory effects for exposure to electromagnetic fields.

Frequency Range	Specific Absorption Rate in the head (SAR) [mJkg^{-1}]
$0.3 \leq f \leq 6 \text{ GHz}$	10

3. Currents in limbs.

Indirect effects: Effects caused by the presence of an object in an electromagnetic field that could pose a health and safety hazard, including:

- Interference with electronic medical equipment and devices, including pace-makers and other implanted or body-worn medical devices.
- Propulsive risk of ferromagnetic objects within static magnetic fields.
- Initiation of electro-explosive devices (detonators).
- Fires and explosions due to ignition of flammable materials caused by induced fields, contact currents, or electrical discharges.
- Contact currents.

Table 1.7: AV for contact current (Integrated Circuit (IC))

Frequency	Steady-State Contact Current [mA] (RMS).
Up to 2.5 KHz	1.0
$2.5 \text{ KHz} \leq f \leq 100 \text{ KHz}$	0.4 f
$100 \text{ KHz} \leq f \leq 10000 \text{ KHz}$	40

1.3.3 Hazards of Electromagnetic Radiation to Fuel

The **HERF** refers to risks associated with electromagnetic radiation to fuels and combustible materials. The likelihood of fuel vapor ignition by RF-induced arcs is small, as the following conditions must simultaneously occur for ignition to take place:

- Flammable fuel-air mixture must be present within the range of the induced arc.
- The arc must contain a sufficient amount of energy to cause ignition.
- The space through which the arc occurs must be a certain minimum distance.

The flammability limits of Motor Gasoline (MOGAS) range between 1.25% and 7.6% volume of gasoline vapors in the air. Handling gasoline under normal operating conditions does not create a flammable atmosphere unless near fuel vents, open fuel intakes, or gasoline leaks. Without ventilation, flammable gasoline vapors, being heavier than air, can travel or pool on an inclined surface such as that provided by an aircraft wing or fuselage before dissipating. However, if there is airflow (wind), gasoline vapor is quickly diluted and dispersed, reducing the zone of potential ignition. The flammability of hydrocarbons is also influenced by temperature.

Understanding the risks of HERP, HERO, and HERF is crucial to ensuring the safety of individuals, devices, and materials in the presence of explosions and high-energy electromagnetic exposures. Designing electronics resilient to electromagnetic pulses, implementing safety measures for ordnance, and adopting safe fuel management procedures are essential for mitigating potential hazards associated with these intense electromagnetic phenomena.

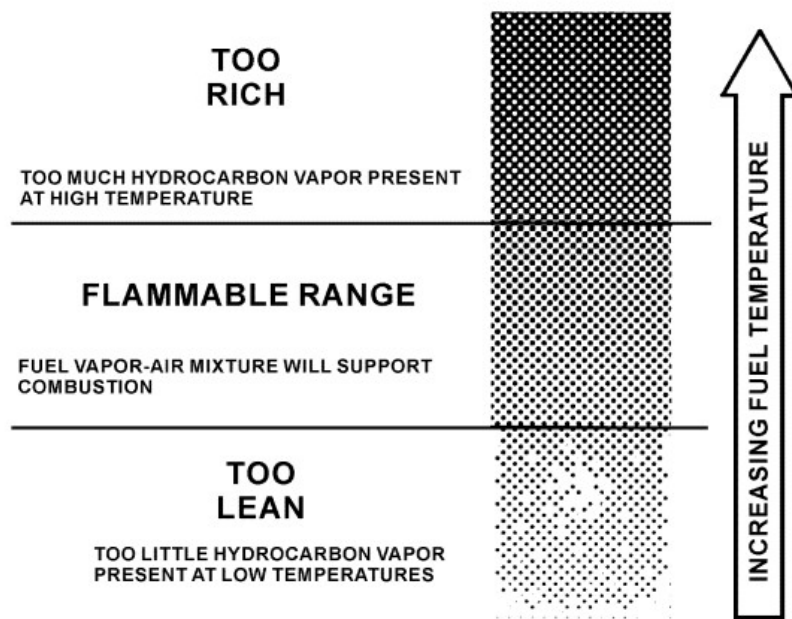


Figure 1.4: Effect on Flammable Fields due to an Increase in Fuel Temperature.

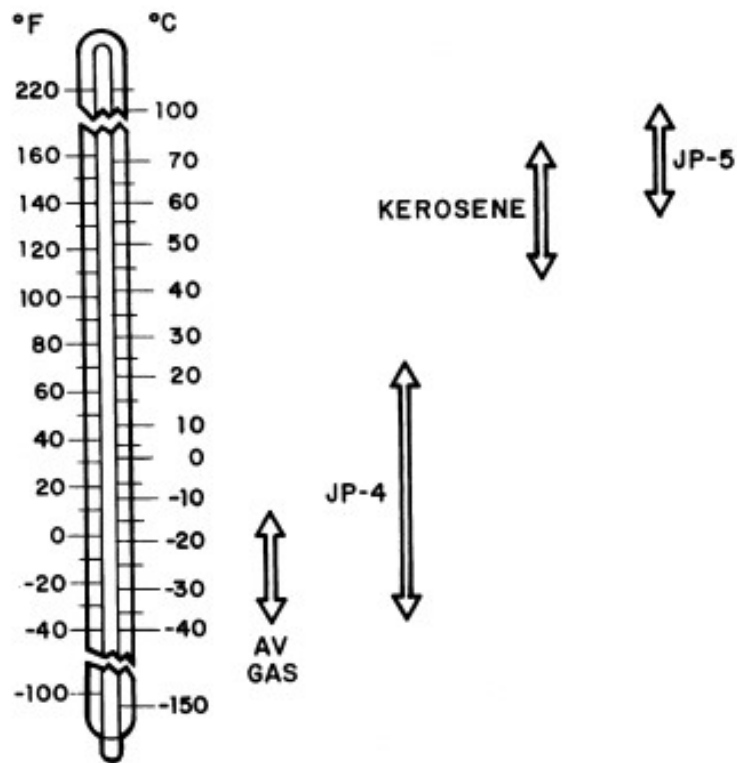


Figure 1.5: Temperature-Flammability Regions for Various Common Fuels.

Chapter 2

Wire Antennas

An antenna [13] is a subsystem that acts as an interface between circuits and the surrounding space. Its function is to convert guided electromagnetic energy within circuits into energy that can propagate through free space. This conversion entails a shift in perspective from analyzing voltages, currents, and powers to studying vector quantities such as electric field (\mathbf{E}), magnetic field (\mathbf{H}), and the Poynting vector (\mathbf{S}). These quantities have physical interpretations closely linked to those of the aforementioned electrical properties.

Many types of antennas can be found in the literature or in the market, but they can be roughly grouped in a few categories:

- the aperture antennas, which are extended in two dimensions, usually large with respect to the wavelength (up to thousands of wavelengths); for this reasons, they are used especially at higher frequency (approximately, above around 1 GHz): typical examples of antennas of this type are the horn antennas, the parabolic antennas and others;
- the wire antennas, which are extended essentially in one dimension, usually of small size, very often less than one wavelengths, so that they are used mainly at low frequencies (approximately, below about a few GHz): typical examples of antennas of this type are the dipoles on others derived from it;
- the array antennas, which are sets of radiating elements (of one of the previous two categories) arranged in the space to obtain particular radiation characteristics.

During the development of this thesis work, wire antennas will be specifically addressed, analyzing different types and characteristics.

Wire antennas represent a fundamental category of antennas used in the field of electromagnetic communications. These antennas are comprised of a linear conductor, such as a metal wire or cable, which is used to radiate or receive electromagnetic waves. Due to their simplicity and versatility, wire antennas find extensive applications across various sectors, including telecommunications, broadcasting, telemetry, and many others.

Wire antennas leverage the fundamental principles of electromagnetism to transmit or receive electromagnetic signals. When an electric current flows through the linear conductor, an electromagnetic field is generated around it. This field emits electromagnetic energy into the surrounding environment, enabling signal transmission. Simultaneously, the antenna can receive electromagnetic signals from the surrounding environment, generating an electric current that can be used for reception purposes.

In the analysis and design of wire antennas, several parameters are considered to evaluate their performance. Some of the most significant parameters include:

- Gain: The gain of a wire antenna represents its ability to concentrate electromagnetic energy in a specific direction. It is an indicator of the antenna's directivity and measures the ratio between the power radiated or received in a specific direction and the power that would be radiated or received by a reference antenna. A higher gain indicates greater efficiency in signal radiation or reception. The gain of a dipole antenna depends on the length of the arms and the operating frequency of the antenna. For a loop antenna, the gain depends on the shape and dimensions of the loop.
- Impedance: The impedance of a wire antenna represents the resistance to the flow of electric current in the antenna. It is a fundamental parameter for ensuring proper matching between the antenna and the feeding or receiving system. The impedance of the antenna can be influenced by factors such as the length of the wire, the operating frequency, and the surrounding environment. Adequate impedance matching maximizes the efficiency of signal transmission or reception. In the design of a wire antenna, it is important to consider the characteristic impedance of the wire used and the type of connection between the antenna and the feeding or receiving system.
- Bandwidth: The bandwidth of a wire antenna indicates the range of frequencies over which the antenna can operate efficiently. A wider bandwidth allows the antenna to support a wide range of signals and adapt to different communication needs. The bandwidth of a dipole antenna depends on factors such as the antenna's geometry, conductor material, and feeding design.

To ensure adequate bandwidth, it is necessary to optimize the antenna's geometry and its response across the frequency spectrum.

- Polarization: The polarization of a wire antenna refers to the orientation of the electric field of the electromagnetic wave radiated or received by the antenna. Wire antennas can be vertically polarized, horizontally polarized, or differently polarized, depending on the specific application requirements. Proper antenna polarization is crucial to ensure better signal transmission and reception. The polarization of transmitted and received signals must be compatible between the antenna and the communication or receiving system. The choice of polarization depends on the antenna configuration and the signal characteristics.

Wire antennas have several advantages and disadvantages. Below are listed some of the main ones:

Advantages of wire antennas:

- They are relatively simple to design and construct. They require fewer components and complex structures compared to other types of antennas, making them more accessible even for beginners.
- They are generally less expensive compared to more complex antennas such as panel antennas or parabolic antennas. This makes them a cost-effective choice for many applications.
- They can be easily adapted to operate at different frequencies and meet specific polarization requirements. They are suitable for a wide range of applications, from radio reception to use in wireless communication systems.
- Unlike some larger antennas like high-gain directional antennas, wire antennas can be made in more compact sizes. This makes them suitable for installation in limited spaces or environments where aesthetics is an important factor.
- At low vertical angles, they simply focus on radiation.
- They radiate over any frequency range for which their overall length is not less than $\lambda/2$.

Disadvantages of wire antennas:

- They tend to have lower radiation efficiency compared to more complex antennas. This means that some of the energy is dispersed or absorbed by the antenna structure itself, reducing the overall effectiveness of the communication system.

- They usually have more limited directivity compared to specialized directional antennas such as panel antennas or parabolic reflector antennas. This can affect the ability to efficiently receive or transmit signals over long distances or in certain directions.
- The surrounding environment, such as buildings, trees, and other objects, can significantly impact the performance of wire antennas. The effect of these obstacles can result in reduced quality of received or transmitted signals.
- At low frequencies, the dipole antenna exhibits a large size.
- They require an appropriate matching system and tuning system to achieve better results.

In conclusion, wire antennas offer a simple, versatile, and cost-effective solution for many electromagnetic communication applications. However, they have some limitations in terms of efficiency, directivity, and sensitivity to the surrounding environment. The choice to use a wire antenna will depend on the specific needs of the application and the limitations of the environment in which it is used.

2.1 State of Art

Over the years, various types of wire antennas have been developed, each with unique characteristics and specific advantages. Below, we will elaborate on the state of the art of wire antennas and provide details on some common types of antennas:

- Monopole antenna: A type of radio antenna that includes a straight rod shape conductor that is perpendicularly mounted above a ground plane is known as a monopole antenna. This antenna is a simple and single-wire antenna, mainly used for both transmitting and receiving signals, so broadly used in wireless communication systems.

The working principle of a monopole antenna is: when the power is fed to a monopole then it is radiated similarly in all directions vertical to the antenna's length above the ground plane on which it is mounted. The radiation pattern of this antenna is omnidirectional, so it radiates with equivalent power within all directions at right angles to the antenna. The radiated power from the antenna changes with elevation angle through the radiation dropping off to zero at the peak on the axis of the antenna.

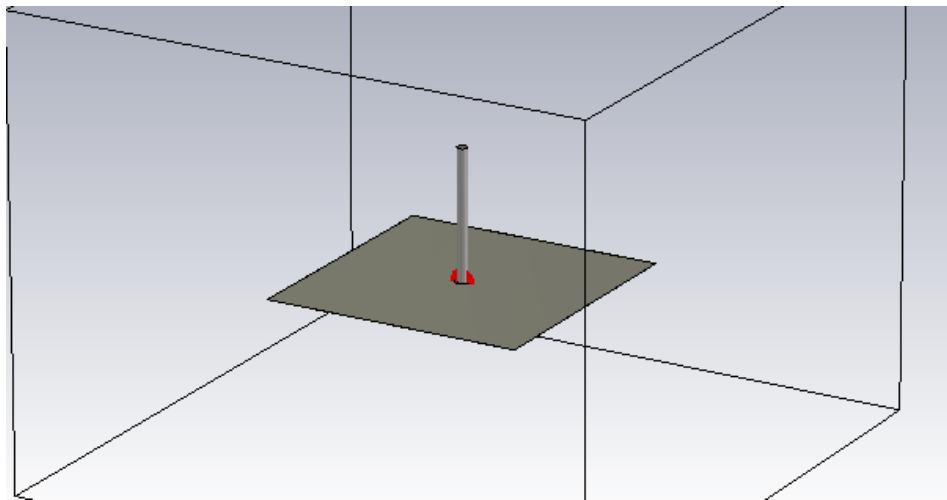


Figure 2.1: Design of Monopole Antenna made with CST-Studio.

- Marconi Antenna: The Marconi antenna is a dipole variant of the classic monopole antenna. It comprises a vertically-oriented rod fed at its base and a ground plane positioned beneath it. By use of the Marconi antenna, which is a quarter-wave in actual physical length, the half-wave operation may be obtained. The Marconi antenna finds extensive applications in long and medium-wave communications, including international broadcasting and long-range maritime communications.

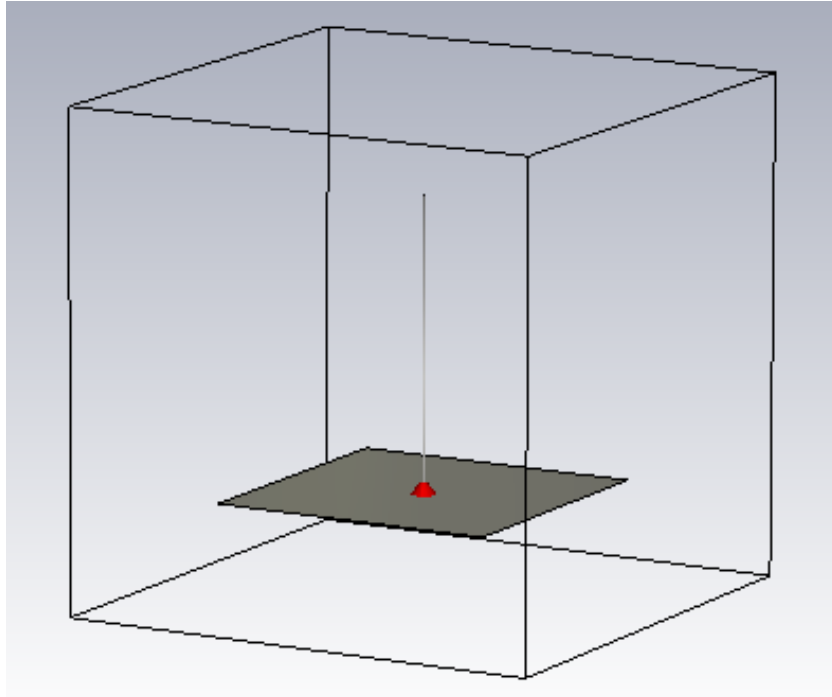


Figure 2.2: Design of Marconi Antenna made with CST-Studio.

- Dipole: The dipole is one of the simplest wire antennas and is widely used in many applications. It consists of two conductive elements through which current flows. This current, along with the associated voltage, allows the radiation of an electromagnetic wave or a radio signal outward. The radiating element of the antenna is divided into two separate conductors, typically aligned on the same axis and with a central division characteristic of a dipole antenna. A transmitter provides the power to irradiate the signal, while in reception, the antenna collects the signal and transfers it to the receiver. Often, an intermediate feeder is used to enable power transfer between the feeding point and the antenna.

The length of the radiating elements plays a crucial role in the characteristics of the dipole antenna, influencing its feeding impedance, central operating frequency, and whether the antenna is resonant or not. Therefore, the dipole's length is a fundamental parameter to consider in the design of these antennas. Dipole antennas are used in many areas, both on their own and as part of more complicated antennas where they can form the main radiating element. They are used in many forms of radio system from two way radio communications links, to broadcasting broadcast reception, general radio reception and very many more areas.

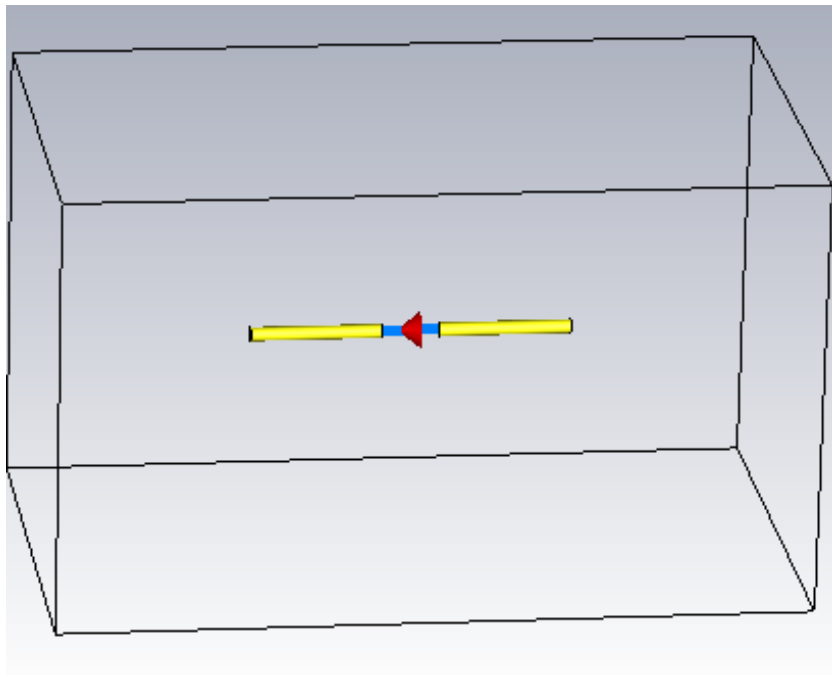


Figure 2.3: Design of Wire Dipole Antenna made with CST-Studio.

- Folded Dipole: The folded dipole antenna is a variation of the conventional dipole antenna. A folded dipole is an antenna, with two conductors connected on both sides, and folded to form a cylindrical closed shape, to which feed is given at the center. The length of the dipole is half of the wavelength. Hence, it is called as half wave folded dipole antenna.

There are two main advantages for using a folded dipole antenna over a standard dipole:

- Increase in impedance: when higher impedance feeders need to be used, or when the impedance of the dipole is reduced by factors such as parasitic elements, a folded dipole provides a significant increase in impedance level that enables the antenna to be matched more easily to the feeder available.
- Wide bandwidth: the folded dipole antenna has a flatter frequency response - this enables it to be used over a wider bandwidth with many transmissions utilising a variety of different selectable channels, e.g. television and broadcast radio, a wide bandwidth antenna is needed. The standard dipole antenna does not always provide the required bandwidth and the additional bandwidth of the folded dipole meets the requirements

The folded dipole antenna finds applications in difference fields, such as long-range communications and maritime radio communication. It is notable for its straightforward construction and consistent performance.

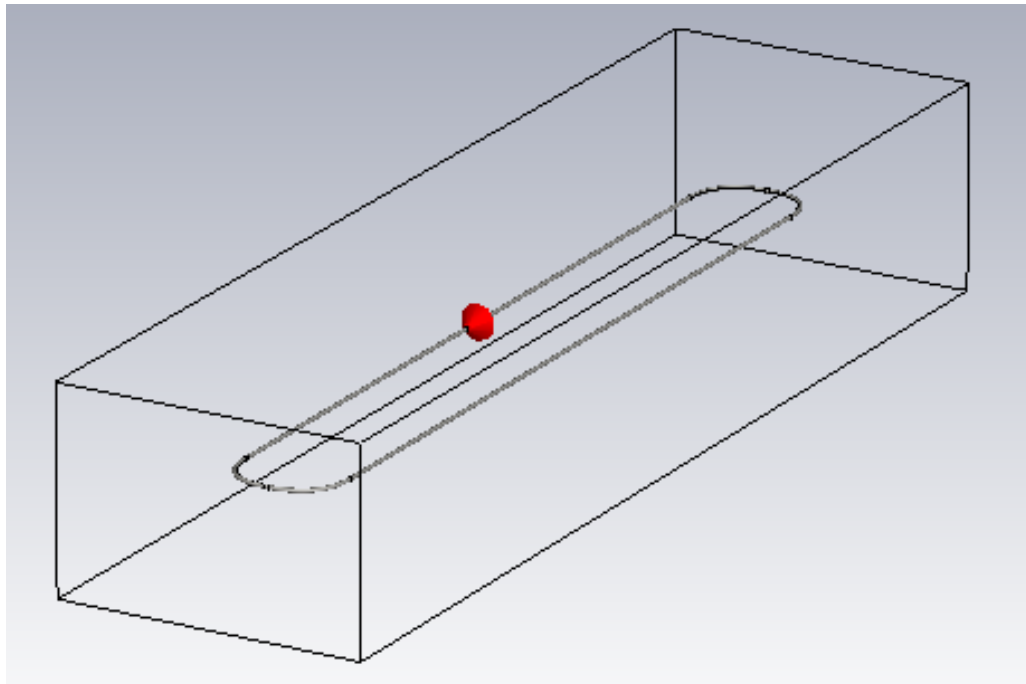


Figure 2.4: Design of Folded Dipole Antenna made with CST-Studio.

- Yagi-Uda Antenna: This antenna consists of a number of parallel dipoles, not all of the same length, but all aligned in a perpendicular way with respect to an axis. Only one of the dipoles is connected to a source and this is called the Driven Element; while all the others are short circuited and are called Parasitic Elements.

Let's analyze the structure: the driven dipole must be in resonance, this condition can be satisfied if each arm has a length equal to $\lambda/4$ where λ depends on the design frequency. Regarding the parasitic elements: typically on one side there is only one parasitic element longer than the resonance length and so with an inductive behavior, indeed it's important to remember that the reactance of the dipole after the resonance frequency becomes positive and for this reason it is inductive; this parasitic element is called Reflector because it has the effect of reflecting the field irradiated by the dipole, which irradiates in all directions, in the direction where are positioned all the other parasitic elements.

On the other side there is a variable number, from about 0 to a maximum of 30 (more or less), of parasitic elements shorter than the resonance length and for this reason they all have a capacitive behavior, indeed the reactance is negative because we are below the resonance frequency; these elements are called Directors and their role is to make more directive the antenna in one specific direction.

In general, in order to design a Yagi-Uda antenna, it's necessary to have a support on which it's possible to put all the elements, this support is a metallic line that can be connected to all the elements in the points in correspondence of which there is zero voltage.

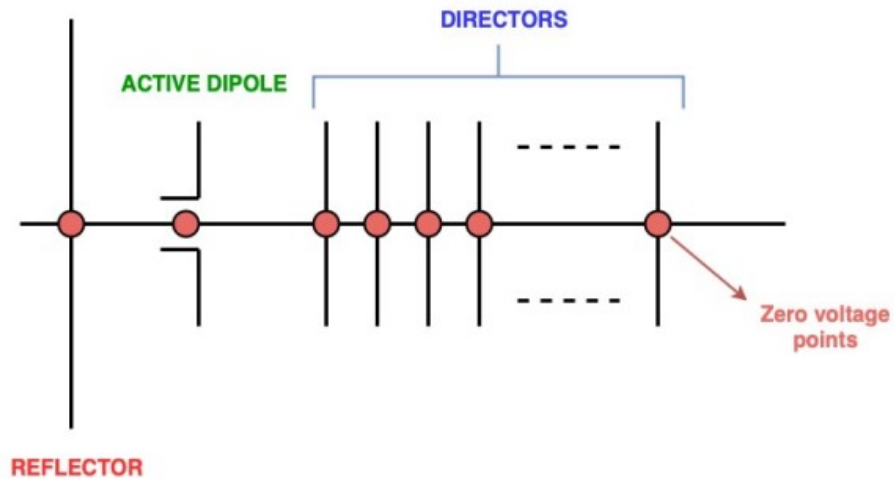


Figure 2.5: Yagi-Uda antenna.

Overall, wire antennas provide a versatile and efficient solution for wireless communication and signal reception. Their design flexibility, ease of implementation, and ability to cover a wide range of frequencies make them an essential component in diverse applications, ranging from broadcasting to telecommunications, scientific research, and beyond. Ongoing research and continuous advancements are further enhancing the performance and capabilities of wire antennas, ensuring their relevance in the continuously evolving field of wireless communications.

Chapter 3

Numerical simulations

3.1 Software Computer Simulation Technology Studio Suite 2022

Within the realm of electromagnetic engineering and antenna design, the utilization of simulation software assumes a preeminent role in the analysis, comprehension, and optimization of intricate electromagnetic phenomena. Among the widely acknowledged and extensively employed simulation platforms, the software CST emerges. This software platform distinguishes itself through a constellation of features that render it an indispensable ally in the process of antenna design and analysis.

The CST software [14] presents itself as a hallmark tool for the simulation and evaluation of antenna performance, offering a three-dimensional and meticulously detailed insight into electromagnetic interactions. This attribute assumes particular significance within antenna design, as it permits the visual exploration of effects stemming from geometric configurations and current distributions, thus affording a comprehensive understanding of key parameters such as radiation, directivity, and impedance.

At the core of CST lies its proficiency in adopting sophisticated simulation methodologies, such as the Perfect Boundary Approximation (PBA) method, the Finite Integration Technique (FIT) algorithm, and the Thin Sheet Technique (TST), to intricately analyze antennas and their interactions within the surrounding environment. This flexibility empowers engineers to scrutinize diverse facets of antennas, ranging from performance under ideal conditions to the scrutiny of realistic and intricate scenarios, encompassing the effects of conductive and dielectric surfaces.

A salient strength of the software is its capacity to model materials with complex electromagnetic properties. This proves pivotal when designing antennas for real-world contexts, where materials may exhibit non-linear responses and dispersion phenomena. The integration of advanced material models into CST facilitates the accurate reflection of electromagnetic field-material interactions, thus yielding results that align meticulously with real-world behavior.

3.1.1 CST Environment

The evolution of electronic technologies has necessitated a more precise understanding and prediction of the behavior of electronic devices and communication networks. The CST Environment within the CST software is a response to this demand.

A distinctive feature of the CST Environment is its versatility in addressing complex issues across various frequency bands. From radio frequencies to microwaves and beyond, the CST Environment offers a unified simulation platform capable of handling highly diverse scenarios. For instance, engineers can employ CST software to design and optimize antennas operating at different frequencies, ensuring efficient coverage of wireless communications.

The CST Environment not only provides an extensive array of predefined device models but also enables users to create custom models to suit the specific needs of their projects. This flexibility is crucial for tackling unique design challenges and attaining accurate outcomes.

3.2 Electromagnetic modeling

Electromagnetic modeling refers to a process in which mathematical representations and computer simulations of electromagnetic phenomena are created. This approach is essential for understanding and predicting how electromagnetic fields behave in various contexts.

3.2.1 The "Finite Integration Technique" Algorithm

The principal concept of the FIT algorithm revolves around the discretization of electromagnetic field equations using a finite volume approach. This involves subdividing the computational domain into a grid of discrete cells.

Each cell contains averaged electromagnetic field values, enabling the accurate calculation of field derivatives and interactions based on that cell's volume. These discretized field values allow the algorithm to numerically solve Maxwell's equations and simulate various electromagnetic phenomena.

One of the distinctive features of the Finite Integration Technique is its flexibility in handling complex geometries and material interfaces. The algorithm is particularly suited to scenarios involving intricate structures and sharp material transitions. This capability is crucial in situations where traditional analytical methods might prove inadequate due to the complexity of the problem. By discretizing space into cells, it provides a means to effectively capture variations in electromagnetic fields across irregular shapes and interfaces. At each time step, FIT updates the electromagnetic field values in each cell, considering interactions between electric and magnetic fields, as well as the material properties within the cell.

In the context of antenna design, the FIT algorithm proves particularly advantageous for modeling electromagnetic radiation, diffraction, scattering, and propagation. These phenomena are critical to understanding antenna behavior and performance. FIT excels at capturing the intricate interactions between antennas and the surrounding environment, rendering it an essential tool for optimization.

3.2.2 The Perfect Boundary Approximation (PBA) method

PBA refers to a proprietary technology that allows to accurately represent arbitrarily curved geometrical features in the model without resorting to any geometrical simplifications. In particular, it helps to avoid the geometrical simplifications typically incurred by the staircase approximation. The staircase approximation results because in most time domain technique, a given mesh cell can only represent the material properties (permittivity, permeability, etc.) of one type of material. Thus, when a mesh cell is partially filled with two different materials, the ambiguity can only be resolved by filling the cell with the material properties of one or the other material; at best, with an average value based on the filling ratio between the two materials.

The PBA works based on the fact that the path for integration (needed for the numerical solution of Maxwell's equations within each mesh cell), can be chosen to conform to the geometry of the object inside the cell, rather than to the edges/faces of the cell itself. In this way, the simulated structure and the electromagnetic fields can be mapped to the hexahedral mesh. This allows a very good approximation of even curved surfaces within the cuboid mesh cells.

3.2.3 The Thin Sheet Technique (TST)

In a sense, TST can be considered as an extension of PBA. If PBA can be used to adapt to the geometry of a given object within a mesh cell, the same concept can be extended to adapt to the geometry of a thin metal sheet within a mesh cell. This allows for an accurate representation of various thin metal sheets without the need to explicitly mesh them with a fine mesh. This has a significant impact on the overall simulation time.

However, it is important to be cautious in a specific situation. Neither PBA nor TST can handle correctly a situation where a mesh cell contains more than two independent non-metallic areas. In this situation, the electric and magnetic fields cannot penetrate the metallic objects and become indeterminate in the space between the metallic objects. Therefore, careful consideration should be given when applying such meshing techniques in complex scenarios involving multiple non-metallic areas within a mesh cell.

3.2.4 The Scattering matrix

The scattering matrix is used to analyze how a multiport device, such as an electronic component, affects electrical signals or electromagnetic waves passing through its ports. It represents how the device reflects, transmits, and interacts with such signals, enabling a detailed analysis of the device's performance.

Lumped circuits

The two-terminal circuit component, as shown in Figure 2.5, is characterized by its impedance Z_L (or its inverse, admittance Y_L), defined as the ratio of voltage V across its terminals to the absorbed current I . Assuming that such an element is linear and that its impedance depends solely on frequency, a pair of terminals of a device is often referred to as a "port." Consequently, this type of circuit component is known as a one-port device. In general, the two voltages V_1 and V_2 depend on both I_1 and I_2 :

$$\begin{cases} V_1 = Z_{11}I_1 + Z_{12}I_2 \\ V_2 = Z_{21}I_1 + Z_{22}I_2 \end{cases} \quad (3.1)$$

Where Z_{ij} is solely a function of frequency.

Meanwhile, equation (3.1) is represented as

$$[V] = [Z][I] \quad (3.2)$$

Where $[V] = [V_1 V_2]^T$, $[I] = [I_1 I_2]^T$ are column vectors, and the 2x2 matrix $[Z]$ is called the open-circuit impedance matrix.

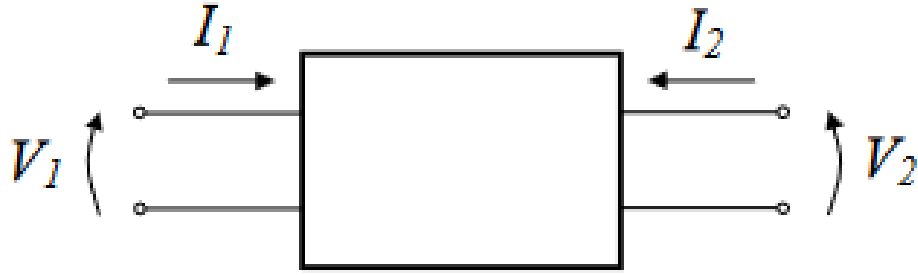


Figure 3.1: Two-port device with the definitions of voltage and current at the ports.

The name is justified by the definition of its elements, derived from (3.1):

$$Z_{ij} = \left. \frac{V_i}{I_j} \right|_{I_k=0, k \neq j} \quad (3.3)$$

In other words, all terminals except the j -th one to which the exciting current is applied must be open circuits. The advantage of matrix notation is that (3.2) can also describe an N -port structure; in this case, $[Z]$ is a complex $N \times N$ matrix. Note that the matrix $[Z(\omega)]$ can be interpreted as a set of transfer functions between the applied currents (input) and the voltages at all terminals (output). The diagonal elements are the input impedances, and the other elements are transimpedances.

As in the case of a one-port device, we can introduce the admittance $Y_L = 1/Z_L$. For an N -port structure, it is possible to introduce a closed-circuit admittance matrix $[Y]$. In the case of $N = 2$, the linear dependence between currents and voltages is expressed as:

$$\begin{cases} I_1 &= Y_{11}V_1 + Y_{12}V_2 \\ I_2 &= Y_{21}V_1 + Y_{22}V_2 \end{cases} \quad (3.4)$$

In matrix form, this can be expressed as:

$$[I] = [Y][V] \quad (3.5)$$

From the comparison with (3.2), we obtain $[Y] = [Z]^{-1}$. The name given to the matrix $[Y]$ derives from the definition of its elements:

$$Y_{ij} = \left. \frac{I_i}{V_j} \right|_{V_k=0, k \neq j} \quad (3.6)$$

In circuit theory, an important role is played by reciprocal and lossless networks.

A circuit composed of resistors, capacitors, inductors, and transmission lines is always reciprocal, meaning it is symmetric in its characteristics. Conversely, an amplifier and devices containing magnetic materials in a static magnetic field are non-reciprocal, and their matrices $[Z]$ and $[Y]$ are not symmetric.

The total power dissipated in the device is the sum of the powers entering through the various terminals:

$$P_{\text{diss}} = \frac{1}{2} \Re\{V_1 I_1^* + V_2 I_2^* + \dots + V_N I_N^*\} = \frac{1}{2} \Re\{N \sum_{i=1}^N V_i I_i^*\} = \frac{1}{2} \Re[V^T [I]^*] \quad (3.7)$$

If the device is lossless, the dissipated power is zero.

Consequently,

$$P_{\text{diss}} = 0 = \frac{1}{2} \Re[V^T [I]^*] = \frac{1}{2} \Re[V^T [Y]^* [V]^*] \quad (3.8)$$

Due to the arbitrariness of $[V]$, it is deduced that

$$\Re[Y]^* = 0 \quad (3.9)$$

Consequently, the matrices $[Y]$ and $[Z]$ of lossless devices are purely imaginary. Another important matrix characterization of two-port devices is based on the equations that relate the input and output voltages and currents of a device:

$$\begin{cases} V_1 &= CV_2 + BI_2 \\ I_1 &= CV_2 + DI_2 \end{cases} \quad (3.10)$$

Distributed parameter circuits

Assuming now that each port "i" of an N-port device is connected to a transmission line with characteristic impedance $Z_{\infty i}$ and propagation constant k_i , it can be noted that the electrical state of a transmission line is usually defined by specifying the amplitudes of forward and backward waves, i.e., V^+ and V^- . Therefore, the description of a one-port device connected to a line is more convenient in terms of reflection coefficient rather than impedance or admittance.

In general, when considering N-port networks, a scattering matrix known as the matrix $[S]$ is introduced. In this formulation, the amplitudes of forward and backward waves on the line are defined as power wave amplitudes, represented as "a" and "b," rather than voltages or currents. This choice is justified by considering the equation representing the net active power in a line with real characteristic impedance.

$$P_t = \frac{1}{2} Y_{\infty} |V^+|^2 - \frac{1}{2} Y_{\infty} |V^-|^2 \quad (3.11)$$

The representation in terms of power is more suitable for analyzing the energy behavior of devices and circuits, enabling a more intuitive understanding of the transmissions and reflections of electromagnetic waves within the system.

Defining:

$$a = Y_\infty V^+, \quad b = Y_\infty V^- \quad (3.12)$$

The equation can be reformulated as:

$$P_t = \frac{1}{2}|a|^2 - \frac{1}{2}|b|^2 \quad (3.13)$$

Therefore, it is evident that "a" and "b" are directly related to the power flow. It is important to note that the dependence on the coordinate "z" of the signals "a" and "b" follows the same dynamics as "V₊" and "V₋":

$$a(z) = a(0)e^{-jkz}, \quad b(z) = b(0)e^{jkz} \quad (3.14)$$

Moreover, there is a relationship between "b(z)" and "a(z)" defined as:

$$b(z) = \Gamma(z)a(z) \quad (3.15)$$

Where " $\Gamma(z)$ " is the local reflection coefficient. This definition of power waves allows describing incident and reflected waves independently of the orientation of the "z" axis, which is arbitrary. Note that the characteristic impedance of the line plays the role of the reference impedance against which the reflection coefficient is calculated.

Generalizing these principles to the context of an N-port device, labeled with the subscript "i = 1,2...N," each port is assigned a reference impedance Z_{r_i} that can be interpreted as the characteristic impedance of a transmission line connected to the port. On this line, power waves " a_i " and " b_i " are defined as follows:

$$a_i = Y_r^i V_i^+, \quad b_i = Y_r^i V_i^- \quad (3.16)$$

In the case of a two-port device:

$$\begin{cases} b_1 &= S_{11}a_1 + S_{12}a_2 \\ b_2 &= S_{21}a_1 + S_{22}a_2 \end{cases} \quad (3.17)$$

This implies that the reflected waves on different lines generally depend on the incident waves on all ports. Introducing the column vectors $[a] = [a_1 a_2]^T$ and $[b_1 b_2]^T$, equation (3.17) can be expressed in matrix form as follows:

$$[b] = [S][a] \quad (3.18)$$

Where $[S]$ is a complex 2×2 matrix, commonly referred to as the scattering matrix. The elements of this matrix are defined as follows:

$$S_{ij} = \left. \frac{b_i}{a_j} \right|_{a_k=0, k \neq j} \quad (3.19)$$

In the characterization of N-port devices through the scattering matrix $[S]$, the elements on the main diagonal represent the typical reflection coefficients at port "i" when all other ports are terminated with their respective reference impedances. The elements off the main diagonal are known as transmission coefficients from port "j" to port "i."

This representation is widely used in microwave applications as it is suitable for high-frequency conditions where voltage and current may not be well-defined quantities. Additionally, it is preferred for the broadband characterization of devices since it is easier to construct broadband matched loads compared to open circuits used in the $[Z]$ matrices.

Relationship between $[S]$ and $[Z]$ or $[Y]$

In equation 3.19, an explicit definition of the elements of the matrix $[S]$ was provided.

Starting from the device characterization in terms of the matrix $[Z]$:

$$[V] = [Z][I] \quad (3.20)$$

Expressing $[V]$ and $[I]$ in terms of power wave amplitudes $[a]$ and $[b]$:

$$[V] = [V^+] + [V^-] = [Z_r]^{1/2}([a] + [b]) \quad (3.21)$$

and

$$[I] = Y_\infty([V^+] - [V^-]) = [Y_r]^{1/2}([a] - [b]) \quad (3.22)$$

Where $[Z_r]$ is the diagonal matrix constructed with the reference impedances of all ports. Remembering that $[Z_r]^{1/2}$ is the diagonal matrix with values $\sqrt{Z_{ri}}$ on the main diagonal. Substituting into (3.20):

$$[Z_r]^{1/2}([a] + [b]) = [Z][Y_r]^{1/2}([a] - [b]) \quad (3.23)$$

Expanding the products and factoring $[Z_r]^{1/2}$ from both sides, we get:

$$[Z_r]^{1/2}([Y_r]^{1/2}[Z][Y_r]^{1/2} + [1])[b] = [Z_r]^{1/2}([Y_r]^{1/2}[Z][Y_r]^{1/2} - [1])[a] \quad (3.24)$$

Canceling the common factor $[Z_r]^{1/2}$, the result is:

$$[S] = [\zeta] - [1][\zeta] + [1]^{-1} \quad (3.25)$$

Where $[1]$ is the identity matrix of size N , and $[\zeta]$ is the normalized open-circuit impedance matrix of the device:

$$[\zeta] = [Z_r]^{-1/2}[Z][Z_r]^{-1/2} \quad (3.26)$$

The inverse relation of (3.25) is:

$$[Z] = [Z_\infty]^{1/2}([1] + [S])([1] - [S])^{-1}[Z_\infty]^{1/2} \quad (3.27)$$

Similarly, the following relations between the scattering matrix $[S]$ and the short-circuit admittance matrix can be obtained:

$$[S] = [1] - [y][1] + [y]^{-1} \quad (3.28)$$

Where the normalized admittance matrix is defined as:

$$[y] = [Z_r]^{1/2}[Y][Z_r]^{1/2} \quad (3.29)$$

The inverse relation is:

$$[Y] = [Z_\infty]^{-1/2}([1] - [S])([1] + [S])^{-1}[Z_\infty]^{-1/2} \quad (3.30)$$

Computation of the power dissipated in a device

Continuing to consider an N -port device characterized by its scattering matrix $[S]$, the power dissipated in it is the sum of the net active powers flowing in all ports

$$P_d = \frac{1}{2} \sum_{i=1}^N (|a_i|^2 - |b_i|^2) = \frac{1}{2} ([a]^T \cdot [a] - [b]^T \cdot [b]) \quad (3.31)$$

Now, recalling that:

$$[b] = [S][a], \quad [b]^T = [a]^T [S]^T \quad (3.32)$$

so:

$$P_d = \frac{1}{2} [a]^T ([1] - [S]^T [S]) [a] \quad (3.33)$$

It is evident how this equation, for a one-port device ($N = 1$), reduces to:

$$P_d = \frac{1}{2} \frac{|V^+|^2}{Z_\infty} (1 - |\Gamma|^2) \quad (3.34)$$

Where $|V^+|$ is the magnitude of V^+ and Γ is the reflection coefficient.

Properties of the scattering matrix $[S]$ of a device

A reciprocal device has a symmetric matrix $[S]$, $[S] = [S]^T$; while a lossless device has a unitary scattering matrix, $[S]^T \cdot [S] = [1]$. This follows immediately from (3.33), requiring that $Pd = 0$ for arbitrary excitation $[a]$.

In the case of $N = 2$, the previous equation yields:

$$\begin{aligned} |S_{11}|^2 + |S_{21}|^2 &= 1 \\ |S_{12}|^2 + |S_{22}|^2 &= 1 \\ |S_{11}|^2 + |S_{12}|^2 &= 1 \\ |S_{21}|^2 + |S_{22}|^2 &= 1 \\ S_{11}S_{12}^* + S_{21}S_{22}^* &= 0 \\ S_{11}S_{21}^* + S_{12}S_{22}^* &= 0 \end{aligned}$$

These relationships can be interpreted geometrically: the rows and columns of the unitary matrix $[S]$ form an orthonormal basis in the complex vector space of dimension N .

Regarding devices, a passive device will have a scattering matrix $[S]$ in which all eigenvalues of $[S]^T \cdot [S]$ have a magnitude less than or equal to 1.

On the other hand, an active device will be characterized by a scattering matrix $[S]$ in which at least one eigenvalue of $[S]^T \cdot [S]$ has a magnitude greater than 1.

In conclusion, it is important to note that the eigenvalues of $[S]^T \cdot [S]$ correspond to the squares of the singular values of $[S]$, as explained earlier.

Chapter 4

Numerical Results

In this chapter, the fundamental steps followed in the process of designing a broadband antenna have been explored. All stages, from defining the requirements to choosing configurations, and up to optimizations, will be analyzed. Additionally, the results of simulations conducted to assess the effectiveness of the proposed solutions will be presented.

4.1 Design of HF antenna

To accomplish the following thesis work, the design and simulation software CST-Studio was used. Since the main requirement is to have a device capable of generating high electric fields (HIRF), the CMV-600 series antennas [2], and specifically the CMV-605E model, were taken as reference and inspiration.

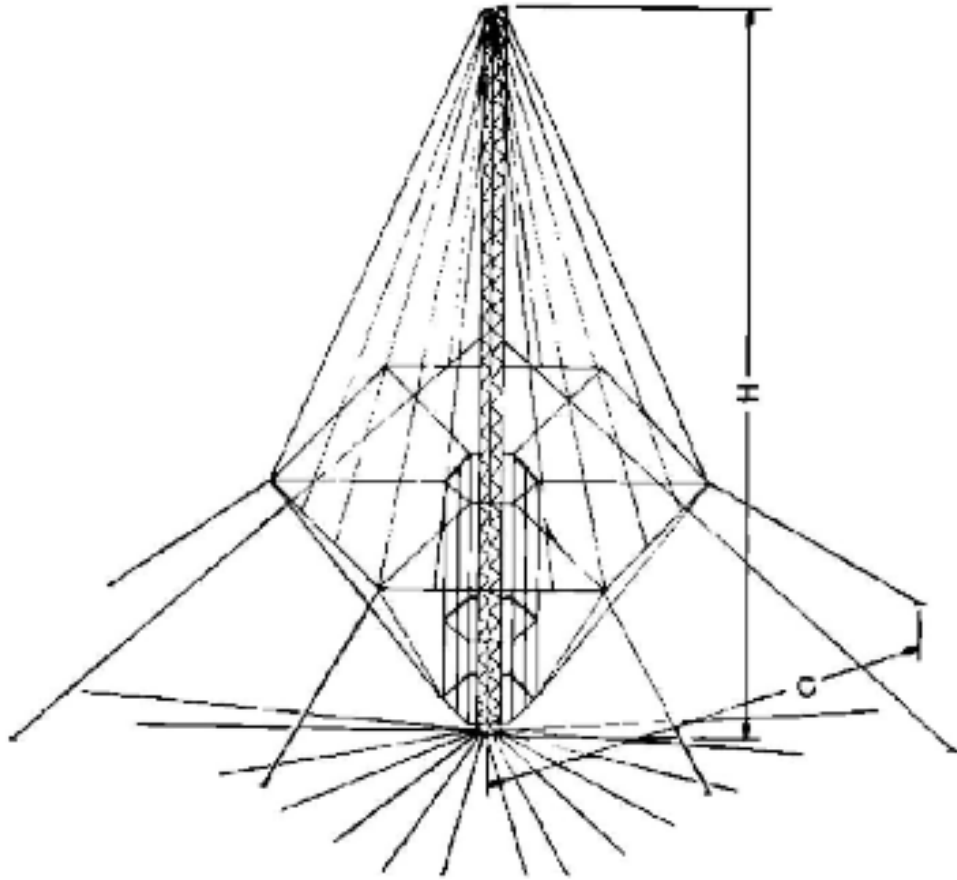


Figure 4.1: Antenna from the CMV-600 series.

During the design phase, before reaching the final design, various preliminary models were developed, playing a crucial role in defining the ultimate configuration of the device.

The first of these models was a vertical monopole antenna (Figure 2.2). This initial step was useful to become familiar with the simulation software and to begin examining the behavior of an antenna within a specific frequency range. However, to address more complex challenges from both a design and performance perspective, it was necessary to proceed further.

Another step involved the implementation of an umbrella antenna (Figure 4.1), which introduced distinct radial elements, giving the antenna a configuration similar to that of an umbrella.

Subsequently, changes were made to the length (L) and the angle of the umbrella's wires. However, upon analyzing the obtained results, it became apparent that this type of antenna exhibited narrowband behavior, which was not in line with the project specifications.

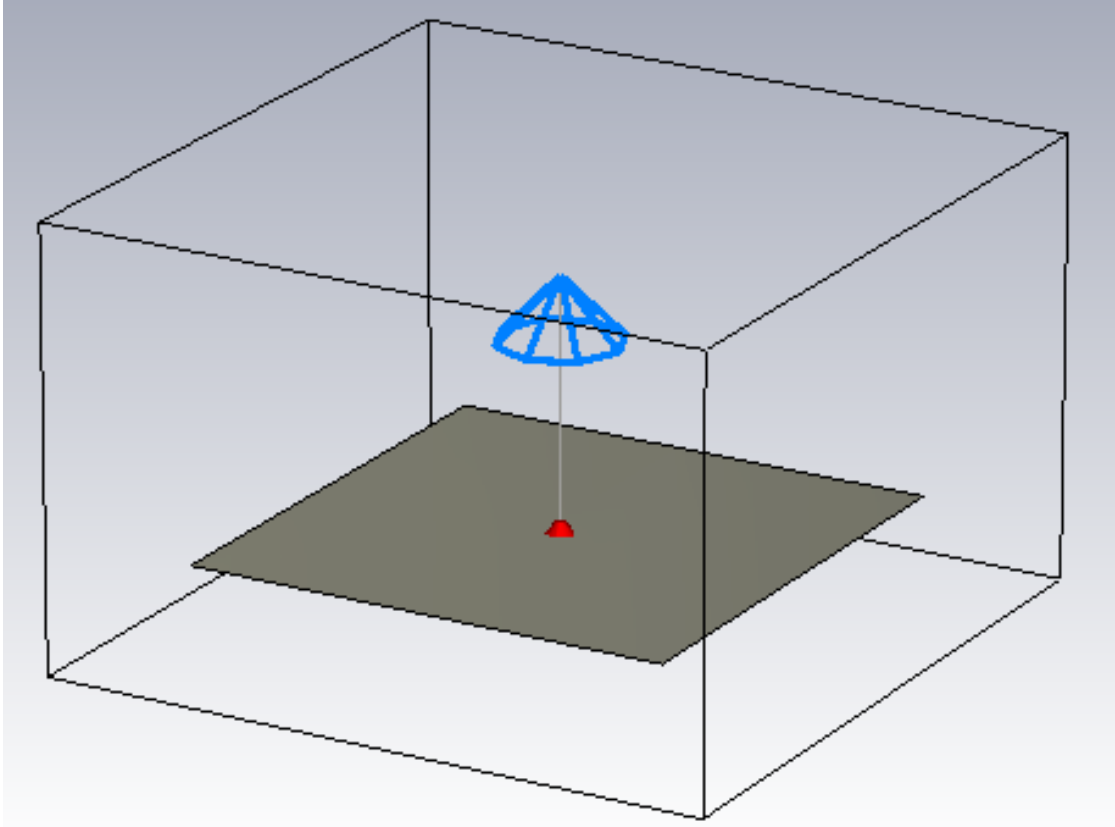


Figure 4.2: Design of an umbrella antenna.

In conclusion, through a careful analysis of the obtained results and the integration of various developed designs, the final antenna with the desired characteristics and behavior was created, approaching as closely as possible the objectives of the SEPRM project.

4.1.1 Design phases

When launching the CST-Studio software, the first step is to create a new project. In this phase, it is necessary to select the application area and the desired workflow.

The choice of the application area defines the specific context in which the software will be used, while the workflow provides a predefined guide for simulations in that context.

Microwave & RF/Optical → Antenna → Wire

The next step involves identifying the solver, defining the units of measurement, and specifying the frequency range in which the antenna must operate. In this specific case, a solver operating in the frequency domain was selected, and a frequency range ranging from 2 to 30 MHz was chosen.

Time Domain → Units → Settings

Once the working window is open, it is possible to start creating the CAD model by precisely defining every aspect of the component, from shape to orientation, to structural details (Figure 4.2).

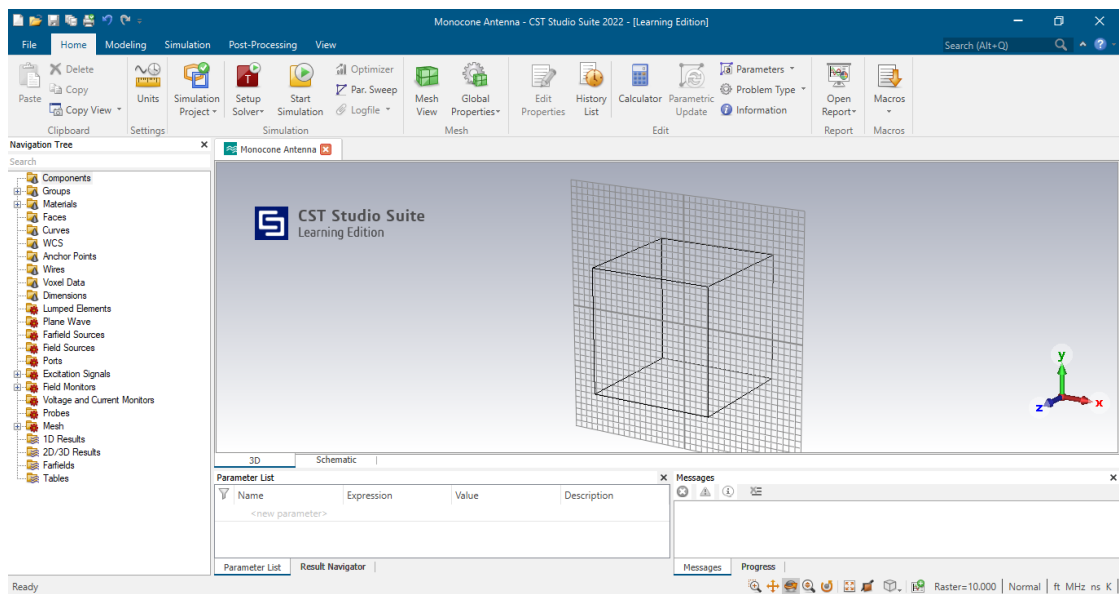


Figure 4.3: Initial working window.

To begin, it is essential to create the ground plane, commonly referred to as "gnd," followed by defining the vertical element that will constitute the monopole.

To perform these operations, you can use the following commands and tools available in the simulator:

Modeling → Brick

In this phase, a window will open that allows you to enter values and define the material for the ground plane of the structure. This configuration will influence the behavior of the "gnd" in the simulation environment, so it is important to input accurate values to obtain precise results in the subsequent phases (Figure 4.4).

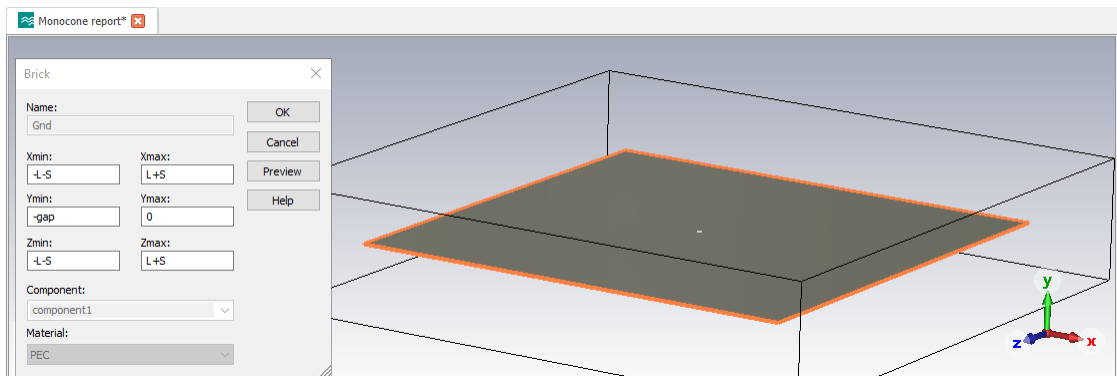


Figure 4.4: Creation of the ground plane.

The same steps were followed to create the vertical element, known as the "Monopole," as shown in Figure 4.5. In this case as well, a dedicated window was opened to input values and define the material for the monopole. This procedure ensures the accuracy and consistency of the antenna model, thus contributing to accurate and reliable simulations in the subsequent stages of the design process.

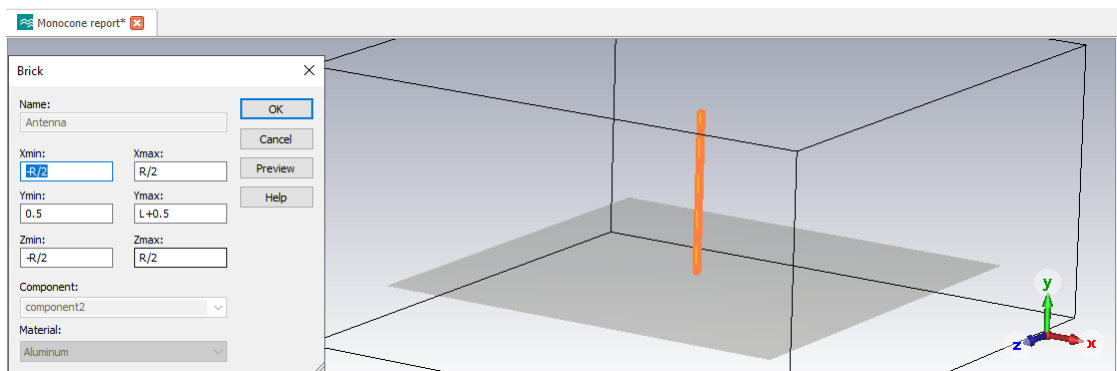


Figure 4.5: Creation of the vertical element.

The next step was the creation of the inverted cone with a hexagonal base surrounding the monopole, as highlighted in Figure 4.6. In the modeling process, particular attention was given to defining the shape and dimensions of the inverted cone. To create this part of the model, the following commands were employed:

Modeling → Bound wire

To create the hexagonal base of the inverted cone, the first segment (wire) was initially defined with zero height. Subsequently, using modeling tools, the initial segment was selected and duplicated using the "Copy" and "Rotate" functions. This operation was performed with a rotation of 60° along the Y-axis, replicating the original segment and creating the remaining sides of the hexagon. This process resulted in the complete hexagonal shape.

Transform → Copy → Rotate

Subsequently, after selecting the entire hexagonal base, a translation was performed upwards to reach a specific height, represented by the variable "X", indicating the height of the inverted cone's base. This operation was carried out using the tools and commands shown in Figure 4.6. The translation action is crucial to correctly position the hexagonal base relative to the antenna's monopole, thereby establishing the precise geometry of the inverted cone in the simulation environment.

Transform → Translate

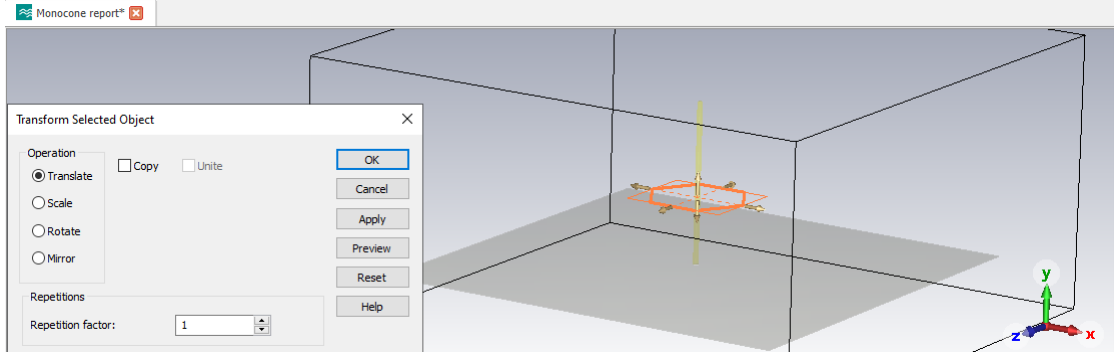


Figure 4.6: Translation of the hexagonal base of the cone.

In the next step, the base was duplicated, and using the "Scale" function, it was reduced in size to create the internal reinforcing structure, as illustrated in Figure 4.7. This operation allowed for generating a smaller version of the base inside the hexagon.

Creating this structure is important to impart stability and robustness to the model, contributing to a better representation of the overall geometry.

Transform → Copy → Scale

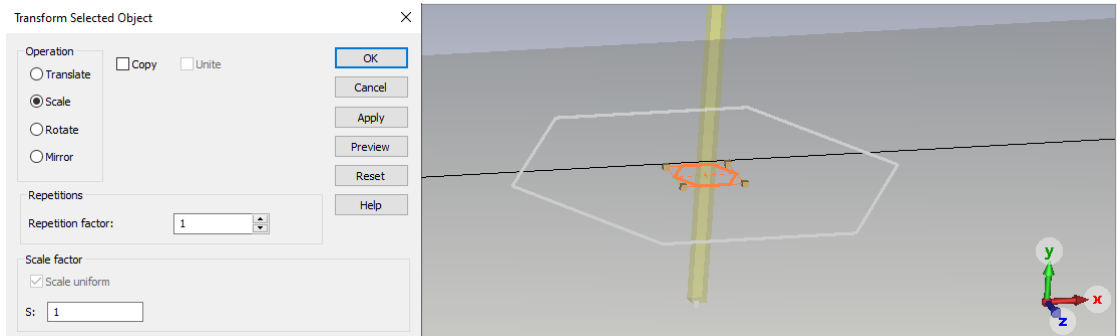


Figure 4.7: Creation of the internal reinforcing structure.

Once the creation of the various structures was complete, it was necessary to establish connections between them. This was achieved through the use of the "Pick end point" function, which highlights two points on the figure, and then using the "bound wire" function to generate the wire that connects these points.

A particular aspect of this design is that the tip of the cone is directly connected to the base of the antenna, as clearly depicted in Figure 4.8. This decision was made after considering two other configurations.

Modeling → Pick end point → bound wire

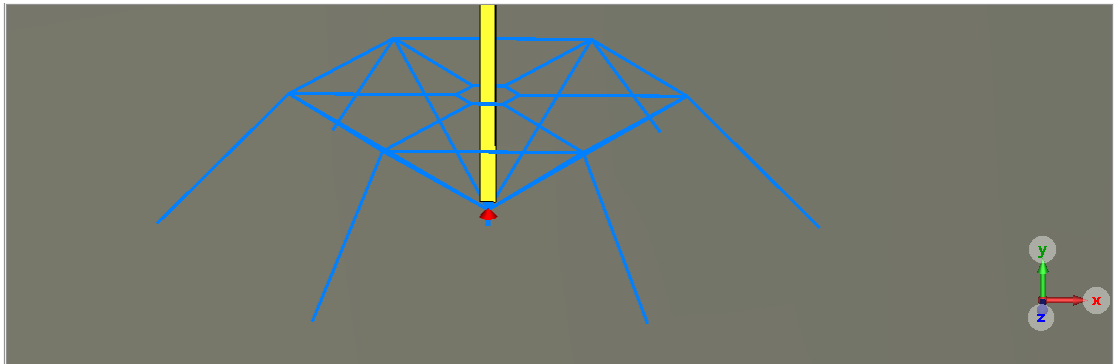


Figure 4.8: Creation of the connecting wires for the conical structure.

A similar operation was performed to connect the tip of the monopole with the base of the cone. This connection was established using the same steps of selecting points and the "bound wire" function. Below, in Figure 4.9, you can observe the complete design of the electronic device.

This design represents the entire model, including the ground plane, the monopole, the inverted cone, and all their respective connections.

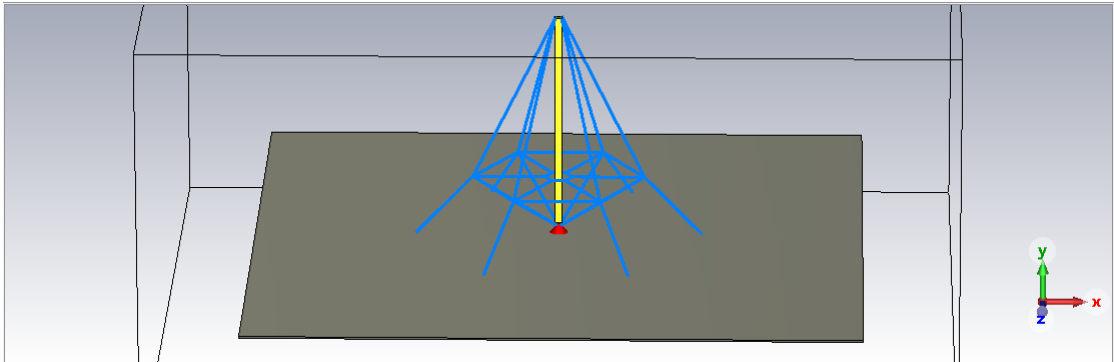


Figure 4.9: Final design of the antenna.

The final phase of the design involves connecting the ground plane "gnd" to the monopole. This connection was made using a "discrete port" in the simulation window, as shown in Figure 4.10.

Simulation → Discrete port → Setup solver

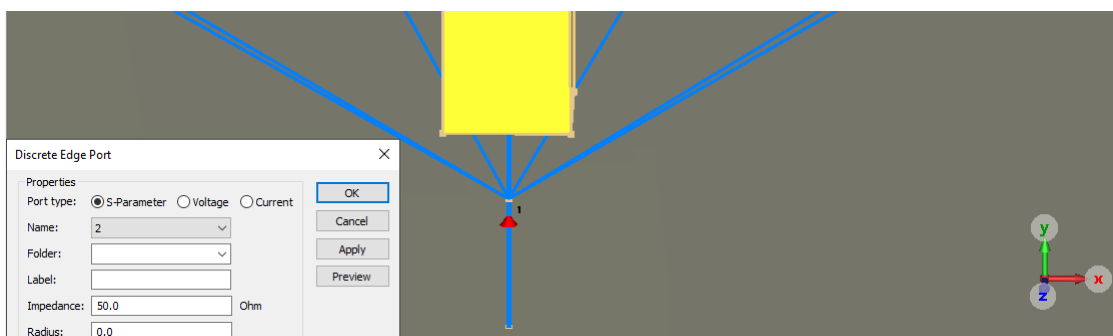


Figure 4.10: Discrete port.

4.2 Simulation and modeling of HF antenna

During the design phase, one of the crucial factors is the accurate selection of dimensions and materials for each component.

The "parameter list"¹, presented in Figure 4.11, provides a comprehensive overview of the key variables used in the system design.

This parameter list offers a detailed compilation of the measurements employed to define the characteristics of each element in the model. The thoughtful choice of these parameters is essential to ensure that the model reliably reflects the behavior of the electronic system under design.

Name	Expression	Value	Description
L	= 36	36	Height
gap	= 0.3	0.3	
R	= 1.12	1.12	Radius
C	= 24	24	Curtain
X	= 10	10	Defines the height of the cone base
P	= 1.2	1.2	Defines the cut tip height of the cone
S	= 15	15	Used to change the size of the Gnd
V	= 0.4	0.4	Defines the size of the cut tip of the cone
F	= 1	1	Define the size of the base of the cone

Figure 4.11: Parameter list.

The choice of materials also plays a fundamental role in ensuring the high performance of the antenna. In the specific context of this work, two materials with distinct characteristics have been adopted.

For the vertical element, the choice fell on aluminum, as illustrated in Figure 4.12. This decision was made considering its excellent properties, including high electrical conductivity, low density, and corrosion resistance. Aluminum is a material of significant relevance in the field of electronics, thanks to its ease of processing, high thermal conductivity, and ability to reflect light. These features make it ideal for electronic components that require energy efficiency and high-performance levels.

¹The size of the length is expressed in feet, a unit of measurement not belonging to the SI

Material to import	
Name:	Aluminum
Type:	Lossy metal
Material sets:	Low Frequency, Default
Attributes:	Description:
Material Set = Default	Chemical symbol: Al
Type = Lossy metal	
Mu = 1	
Electric cond. = 3.56e+007 [S/m]	
Rho = 2700 [kg/m ³]	
Thermal cond. = 237 [W/K/m]	

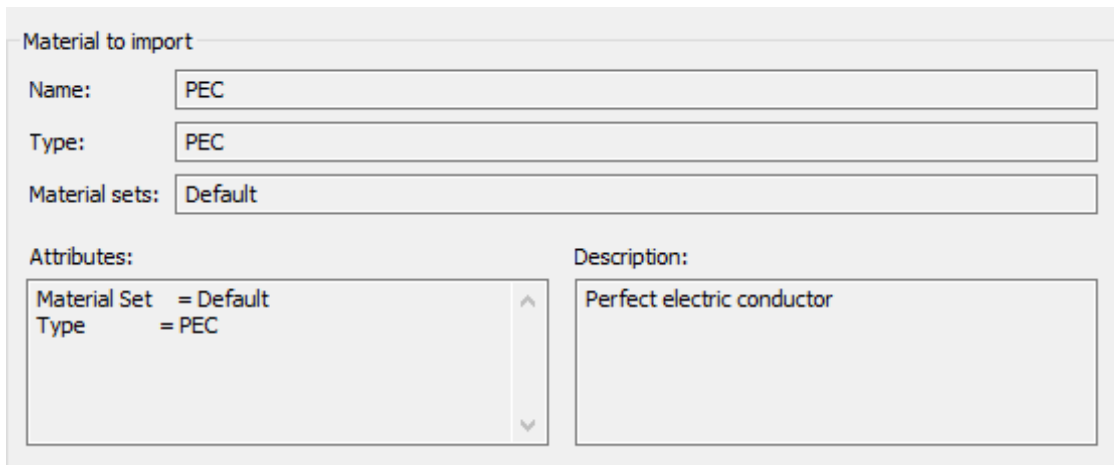
Figure 4.12: Aluminum data sheet.

The ground plane and all wires (wire), on the other hand, are made using a material known as Perfect Electric Conductor (PEC), as indicated in Figure 4.13.

This choice was made because PEC represents an ideal material characterized by two main properties: infinite electrical conductivity and infinite magnetic permeability.

Infinite conductivity implies that PEC conducts electric currents without resistance, behaving like a superconductor.

Infinite magnetic permeability means that PEC completely repels the magnetic field, with field lines unable to penetrate the material but instead deflecting around it.



The image shows a software interface for defining a Perfect Electric Conductor (PEC) material. It is titled "Material to import" and contains several input fields and sections:

- Name:** A text box containing "PEC".
- Type:** A text box containing "PEC".
- Material sets:** A text box containing "Default".
- Attributes:** A scrollable list box containing:
 - Material Set = Default
 - Type = PEC
- Description:** A text box containing "Perfect electric conductor".

Figure 4.13: PEC data sheet.

Once the design phase was completed, the next step was to initiate the solver through the "Setup solver" option. This step marks the transition from the design phase to the simulation phase.

Simulation → Setup solver

With "Setup solver," you configure the settings and parameters necessary for running simulations, allowing the solver to solve the electromagnetic equations that govern the behavior of the antenna and the system as a whole.

4.3 Optimization of HF antenna

With the goal of making the antenna as close as possible to the specified requirements, various design iterations and simulations were conducted. This approach was adopted to generate a wide range of results, allowing for comparisons between different configurations and the selection of the one that best meets the performance requirements.

4.3.1 Different design solutions.

The first step in optimizing the designed system involved analyzing small changes in the design and observing the corresponding results. In this section, two of the considered variants during the design phase will be discussed. This approach emphasizes the importance of an iterative and experimental process to achieve the desired optimal performance in the antenna.

1. The first alternative analyzed is shown in the following figure

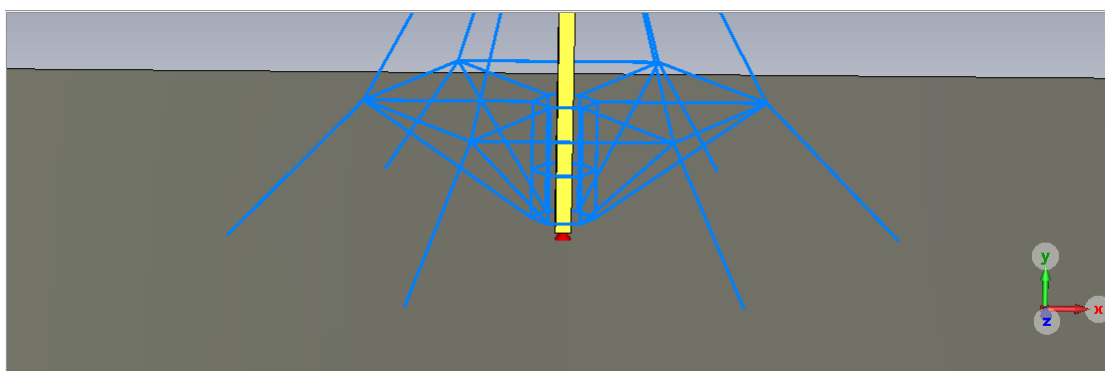


Figure 4.14: First variant: open cone configuration.

In this configuration, the tip of the cone has been cut, and the elements are not directly connected to the feed but are located in proximity to it or capacitively coupled. This design choice introduces a significant variation from the previous configuration (Figure 4.8), as the connections are made more indirectly through capacitive couplings.

2. The second alternative analyzed is shown below.

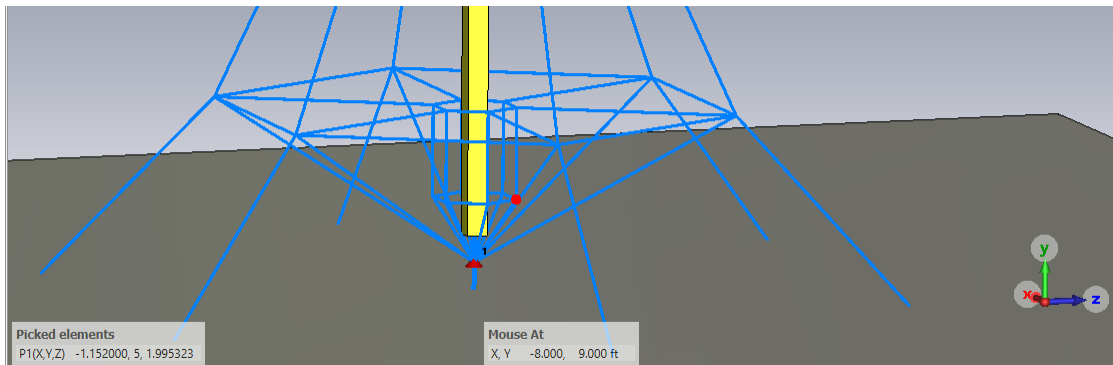


Figure 4.15: Second variant: cone tip configuration with internal structure.

In this second variant, both the cone tip and the internal support structure are directly connected to the base of the antenna. Unlike the first variant, where capacitively coupled connections were used, this option implies a direct connection between the involved parts. This design can lead to significant differences in antenna performance and requires careful analysis to understand the impact of this direct connection on the overall functionality of the system.

In order to determine the optimal configuration for the antenna, a simulation was conducted for each of the different variants considered. In Figure 4.16, shown below, you can observe a direct comparison between the three main analyzed solutions. This visual representation allows for a clear evaluation of performance differences among the various configurations and aids in identifying the solution that best suits the specifications.

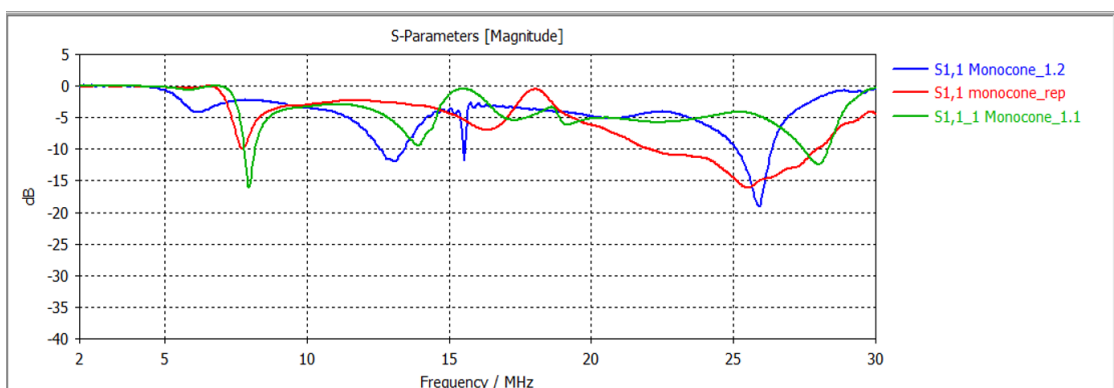


Figure 4.16: S-Parameters plot comparison.

After careful analysis of the various configurations and simulation results, the solution represented in Figure 4.8 was selected, as this design achieved the best broadband performance.

4.3.2 Reference Impedance optimization

The next step was dedicated to finding the optimal value for the reference impedance. As evident from Figure 4.16, the plot shows a broadband response that is not clearly distinguishable, as all curves lie above -10 dB.

Initially, the simulator's default reference impedance, preset to 50Ω , was used. However, to determine the best impedance, the electromagnetic analysis technique called "par. sweep" within the CST software was employed. This approach allowed for systematic variations of the reference impedance to identify the value that produces the most satisfactory performance for the antenna. This optimization phase aims to improve the broadband response of the antenna and achieve more accurate simulation results.

Simulation \rightarrow par. sweep

The "parameter sweep" function allows for an examination of how simulation results vary with changes in model parameters. Initially, relevant parameters to vary are chosen, in this case, the reference impedance. Subsequently, value ranges for each parameter to be examined are defined. The simulator then performs a series of tests, varying the parameters within the specified ranges and collecting data during each simulation. Finally, the collected data is analyzed to understand how the results vary based on the selected parameters.

Figure 4.17 below shows the set of all simulations conducted while varying the reference impedance, from an initial value of 30Ω to a final value of 170Ω .

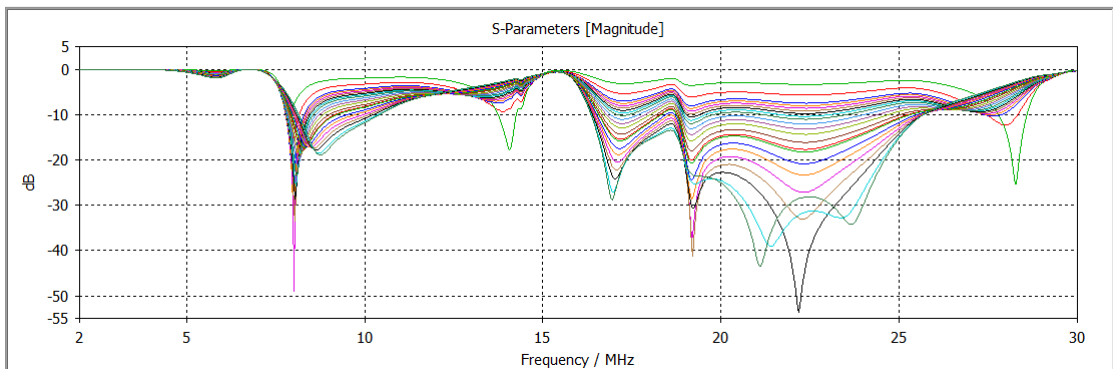


Figure 4.17: Par. Sweep of Reference Impedance

Observing the different curves in the graph clearly reveals that as the reference impedance increases, there is a progressive descent of the response below the -10 dB threshold. This trend demonstrates the desired broadband behavior for the antenna.

In other words, increasing the reference impedance seems to improve the antenna's broadband response, bringing the curves below the -10 dB level over a wider range of frequencies. This phenomenon is of significant importance in antenna optimization, as it indicates a configuration that might better suit the application's needs in terms of broadband performance.

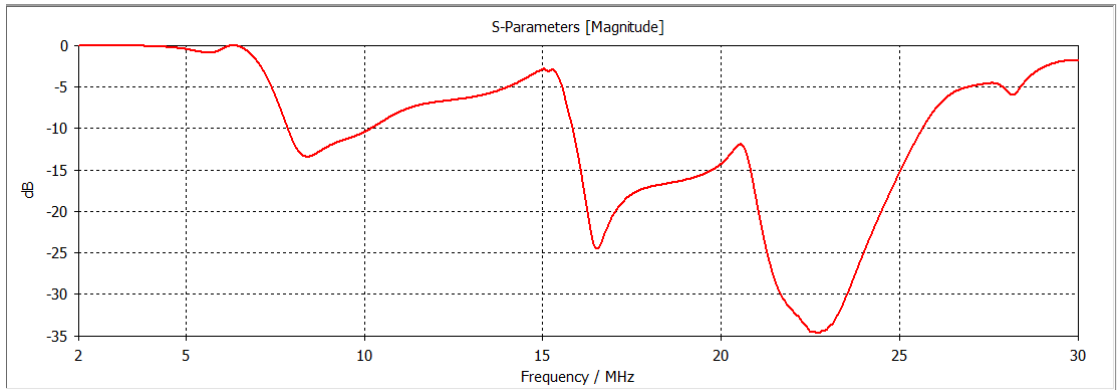


Figure 4.18: S-parameters of the antenna with optimization of the Reference Impedance

Figure 4.18 represents the optimal broadband response achieved, for which the impedance value is assigned as 144Ω . This impedance value has proven crucial in achieving the desired performance.

4.3.3 Optimizer

Once the optimal design and reference impedance were identified, to further optimize the antenna's performance, the CST-Studio Suite software offers the possibility to use the "Optimizer" function,

Simulation → Optimizer → Start

The optimizer (Figure 4.19) is a tool that automates the process of finding the best configuration or set of parameters for a specific device or structure, with the goal of optimizing performance. This function operates through successive iterations, adjusting parameters based on a defined objective. This allows for maximizing antenna efficiency, reducing return loss in a circuit, or increasing the directivity

of a directional antenna. Additionally, constraints can be applied to ensure that optimal solutions are realistic and meet imposed requirements.

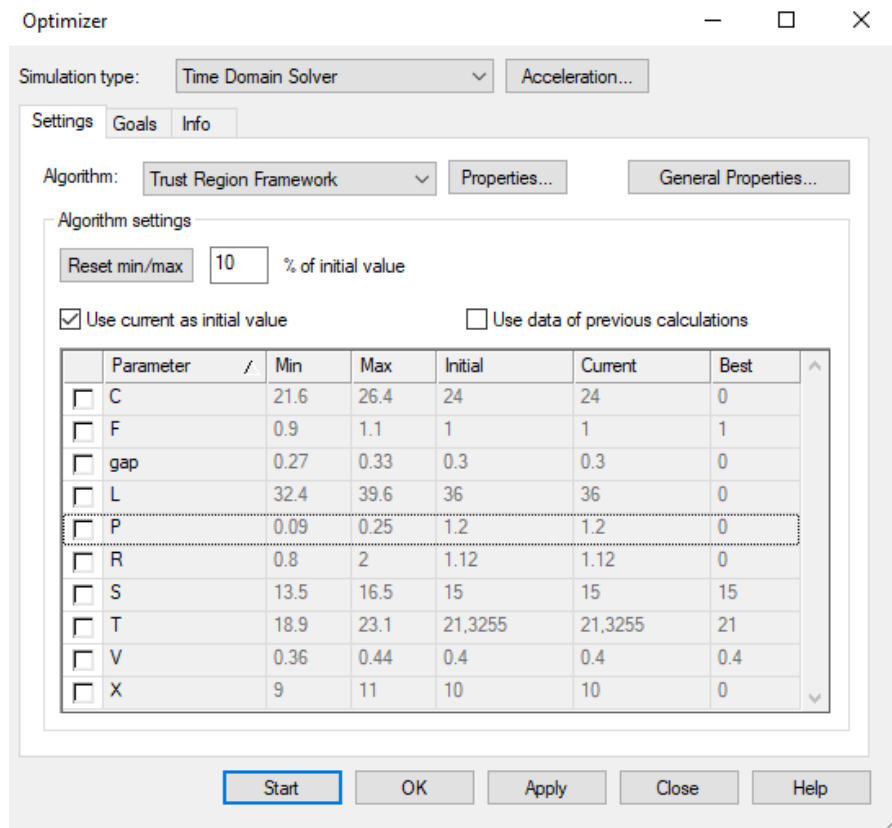


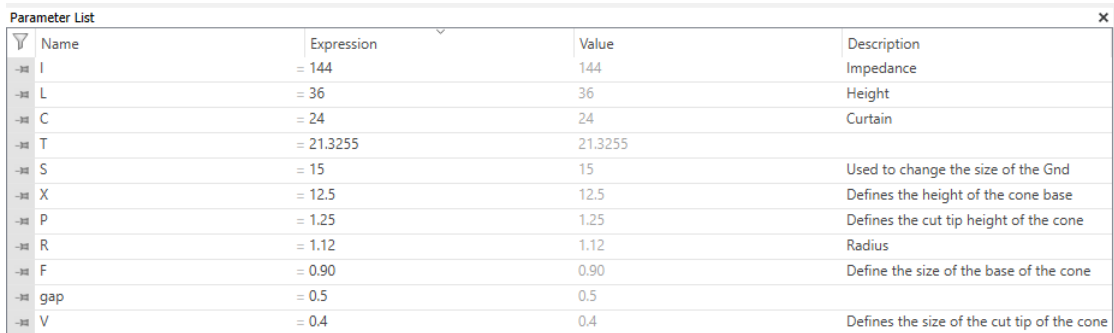
Figure 4.19: Optimizer.

This process was employed for the final selection of crucial key parameters, including:

- Monopole radius (R);
- Ground plane thickness (gnd);
- Monopole height (L);
- Cone base size (S);
- Cone base height (X);
- Inverted cone tip height (P).

These parameters influence radiation properties, bandwidth, and other key characteristics of the antenna. Systematic analysis and optimization of these parameters allow for achieving optimal performance and maximizing antenna efficiency within its intended applications.

Below is the "parameter list"² presented again with the updated values. This list serves as an important resource, reflecting the current state of project parameters and specifications.



Name	Expression	Value	Description
I	= 144	144	Impedance
L	= 36	36	Height
C	= 24	24	Curtain
T	= 21.3255	21.3255	
S	= 15	15	Used to change the size of the Gnd
X	= 12.5	12.5	Defines the height of the cone base
P	= 1.25	1.25	Defines the cut tip height of the cone
R	= 1.12	1.12	Radius
F	= 0.90	0.90	Define the size of the base of the cone
gap	= 0.5	0.5	
V	= 0.4	0.4	Defines the size of the cut tip of the cone

Figure 4.20: New parameter list.

²New list of parameters in which the size of the length is expressed in feet, a unit of measurement not belonging to the SI

4.4 Discussion of results and future developments

4.4.1 Electric Field Values

The analysis of field values in the area surrounding the antenna is one of the main requirements since the fundamental goal is to generate high-power electric fields (HIRF) to conduct necessary tests. Among the various results available from the simulator, there is also the "E-Field" plot, which allows the observation of the electric field's behavior produced by the radiating element. To facilitate the visualization of this analysis, the following sequence of commands has been configured.

Contour → dB → Maximum → Field on a Plane → D

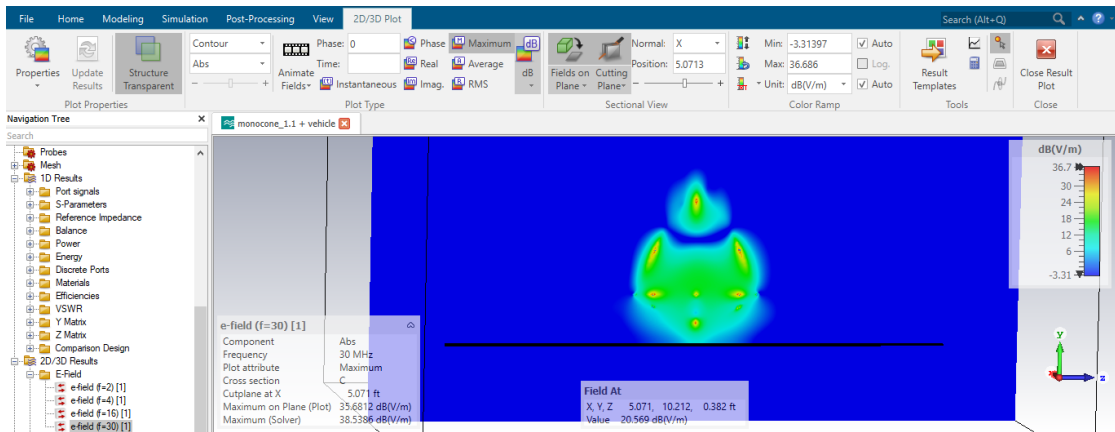


Figure 4.21: E-Field (f = 30 MHz)

The maximum electric field values detected in the initial simulation hover around 37 dB (V/m), a measurement indicative of the use of limited input energy. To refine the analysis further, the subsequent step involved recalibrating the fields through a substantial increase in input energy, concentrated at a frequency of 22.5 MHz. In this configuration, the antenna proves to be exceptionally well-tailored, allowing the entire input power to be effectively absorbed. The outcomes resulting from this recalibration of the fields are intricately depicted in Figure 4.23.

This procedure has proven to be crucial in gaining a deeper understanding of the electric field behavior concerning input power. Such insight allows for a more accurate analysis of the antenna's performance under real feeding conditions.

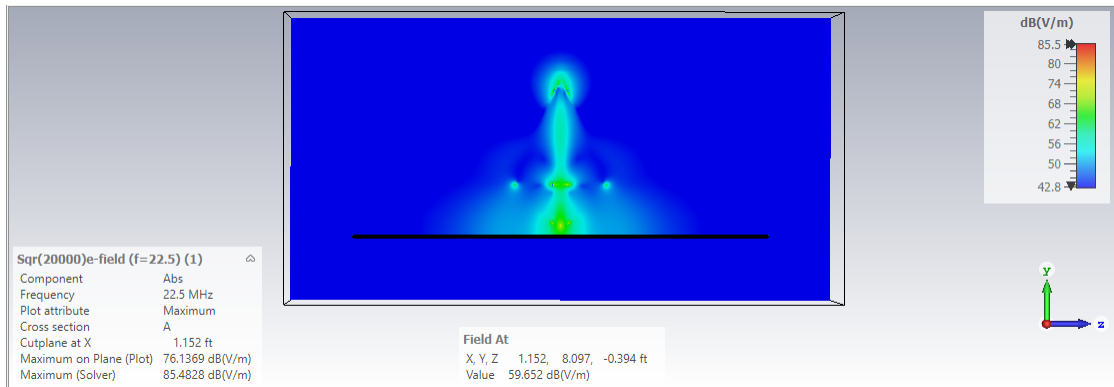


Figure 4.22: Rescaling of the E-Field ($f = 22.5$ MHz) with $X = 0.35$ m

Figure 4.23 unveils recalibrated field values computed at a distance of 0.35 m from the radiating element, showcasing a significantly heightened field compared to that attained in Figure 4.21. Indeed, the detected value at an height of 2,46 m registers at 59.652 dB(V/m). This datum underscores a substantial surge in the electric field concerning the preceding configuration, providing further intricacies regarding the distribution and impact of field recalibration on the antenna.

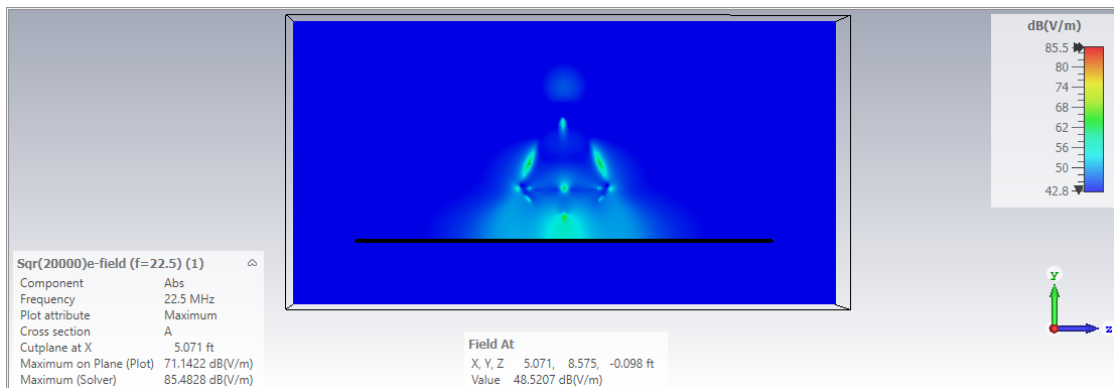


Figure 4.23: Rescaling of the E-Field ($f = 22.5$ MHz) with $X = 1.55$ m

The Figure 4.24, on the other hand, displays the field values obtained at a distance of 1.55 m. From this depiction, a slight decrease in values is noticeable compared to the corresponding height in the previous case. Currently, the value stands at 48.5207 dB(V/m).

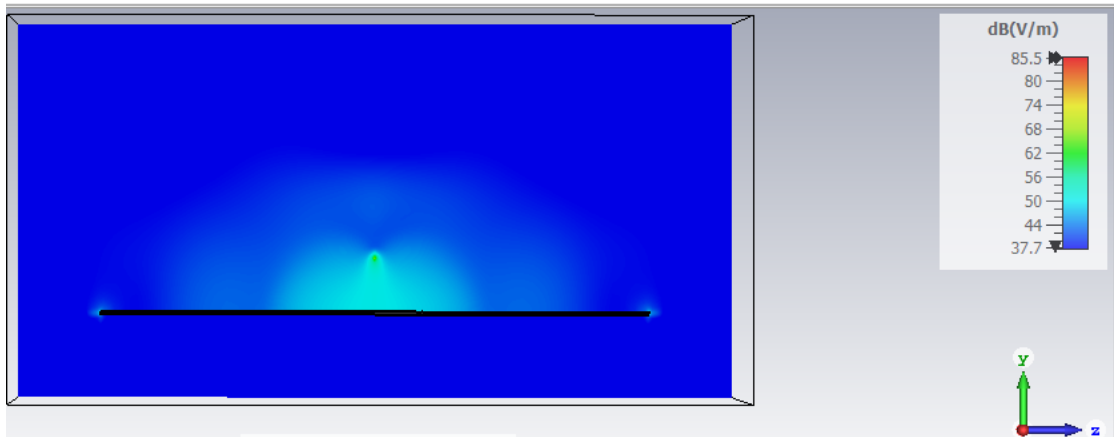


Figure 4.24: Rescaling of the E-Field ($f = 22.5$ MHz) with $X = 4.60$ m

At the end, the graphical representation of the last image highlights the fields at a distance of 4.60 m from the antenna. It is interesting to note that, despite a constant decrease in values, they maintain an overall high and satisfactory level for the test execution. This gradual decrease in values at this distance suggests good efficiency and consistency in the antenna's performance, providing further support for the validity of the conducted tests.

4.4.2 Simulation with the addition of the military vehicle.

To rigorously evaluate the authenticity and effectiveness of the project, an additional crucial test was conducted. In this experimental phase, an additional block of dimensions comparable to those of a military vehicle was introduced. This block was strategically positioned just outside the support structures of the antenna (the guy wires), maintaining a distance of approximately 6 meters from the monopole, as illustrated in Figure 4.25.

The objective of this test was to assess how the system reacts to the presence of a significant obstacle of considerable size in close proximity.

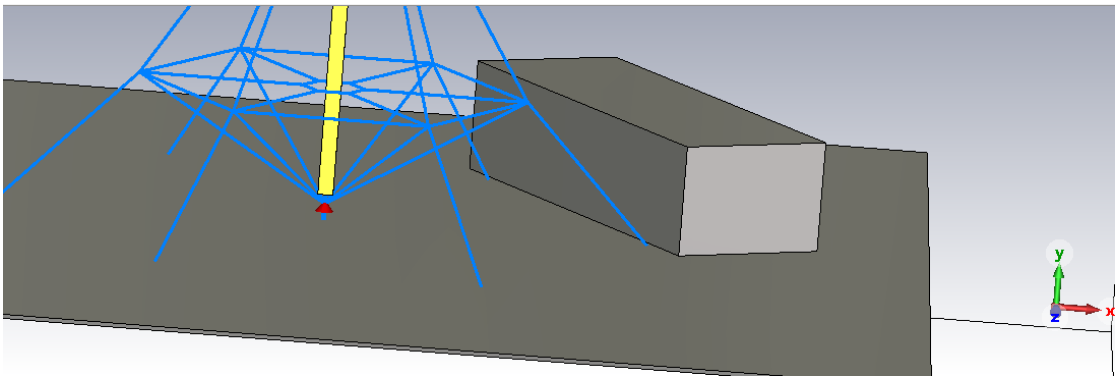


Figure 4.25: Final design with the presence of the vehicle.

This type of simulation is of significant importance due to the specific characteristics of antennas operating at extremely low frequencies, on the order of MHz. In such circumstances, the behavior of an antenna can be significantly influenced by the presence of objects or bodies in its immediate vicinity.

Figure 4.26 presents a direct comparison between two simulations: one conducted in an ideal environment and the other taking into account the presence of the surrounding medium. As expected, the two trends show a remarkable similarity, confirming the system's significant robustness in the presence of an object placed a few meters away. This result highlights the antenna's ability to maintain stable and consistent performance even in proximity to surrounding objects.

This can have positive implications in real-world applications where ensuring communication continuity or survey accuracy is crucial, minimizing the negative effects of external interferences.

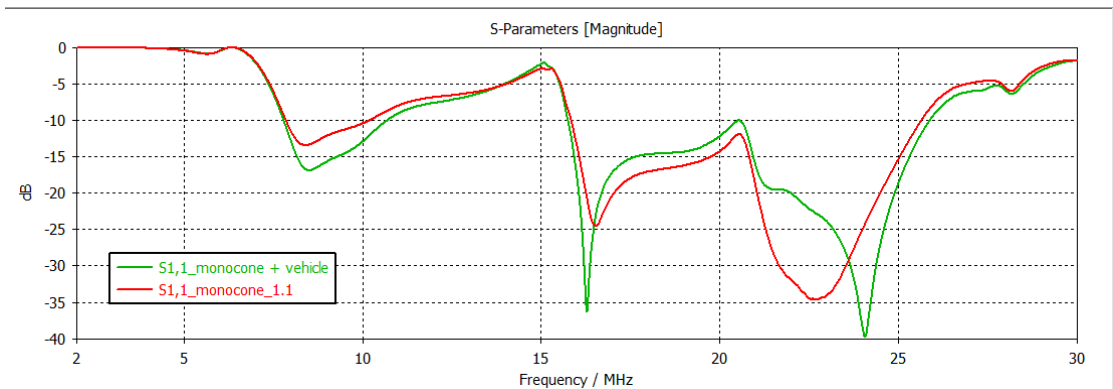


Figure 4.26: Comparison between the ideal simulation and the simulation with the presence of the medium.

Electric field values calculated in a sub-volume

An additional study was conducted, focusing on the analysis of the electric field behavior within a sub-volume having the dimensions of the military medium mentioned in the previous paragraph, as illustrated in Figure 4.27.

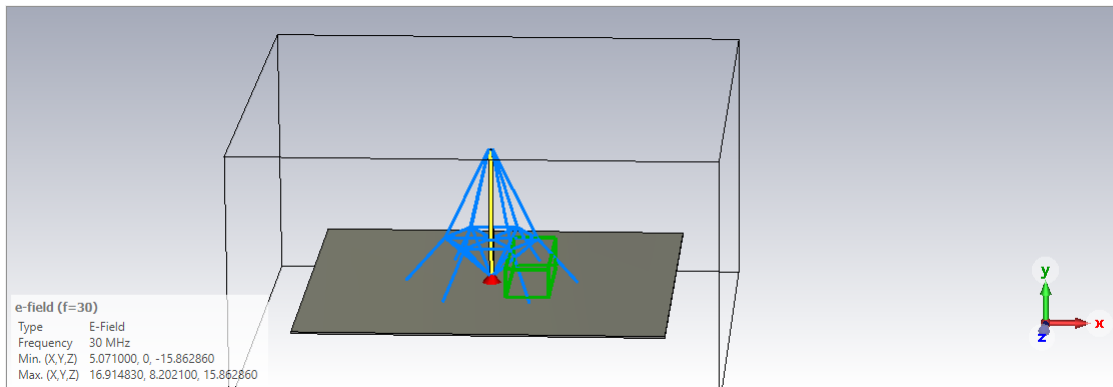


Figure 4.27: Sub-volume Simulation

From the figure, it is evident that the sub-volume is located within the structure, specifically at a distance of 1.55 m from the monopole, even through the guy wires. It is important to emphasize that this representation is purely hypothetical and does not correspond to a real-world situation. The objective of this study is to analyze the radiation not over the entire area surrounding the HF antenna, as analyzed in Figure 4.21, but only within the selected volume, in order to assess whether the electric field values are satisfactory.

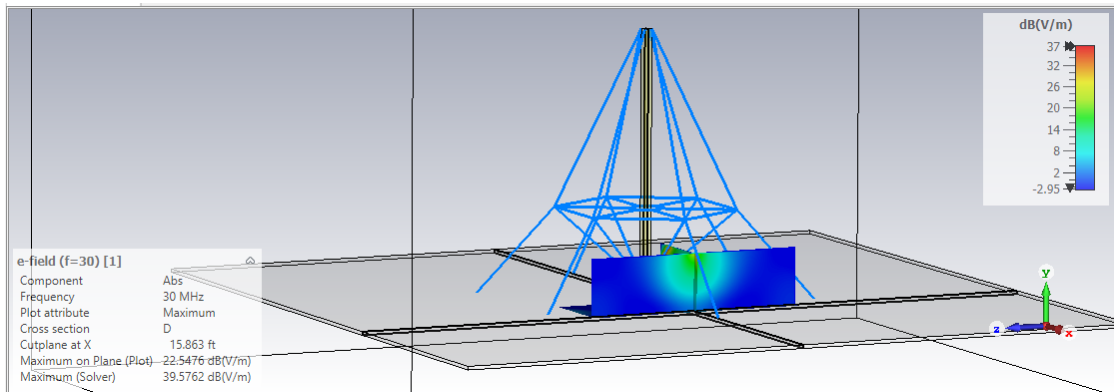


Figure 4.28: Simulation of the sub-volume.

Figure 4.28 presents the results of the simulation and the electric field plot within the sub-volume. This in-depth analysis allows for a better understanding of how the electric field behaves in this specific region, providing crucial information for evaluating the system's adequacy for the desired performance.

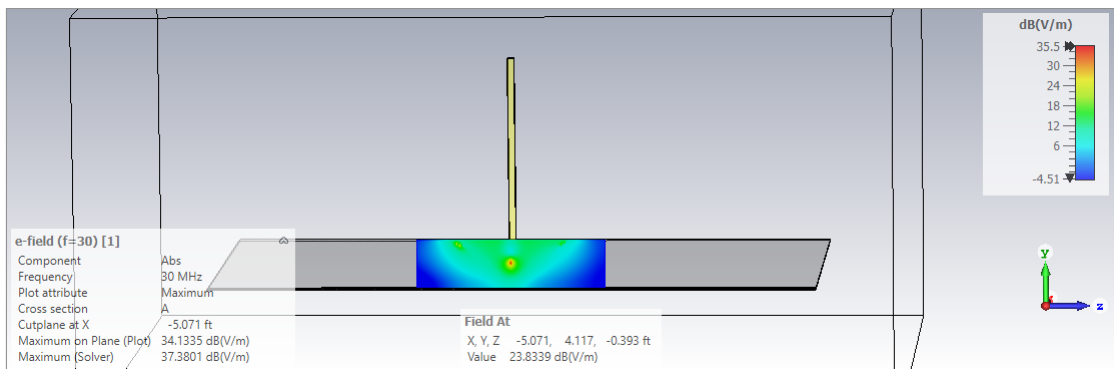


Figure 4.29: Frontal view simulation of the sub-volume.

As highlighted in Figure 4.29, the field values are significantly high and practically occupy the entire volume, only losing some of their intensity at the lateral ends. This phenomenon of electric field distribution provides a clear insight into the authenticity of the design.

Chapter 5

Conclusions

From the in-depth analysis of all the work carried out, it is clear that the design of a radiating device is a complex and not immediate process. To achieve satisfactory results, it is necessary to address a series of challenges, including the detailed analysis of fundamental parameters, the design of different design variants, and numerous simulations. It is evident that to achieve significant results, a comprehensive and rigorous approach is required, with the dedication of time and energy to the analysis of the variables involved and the experimentation of creative solutions. Only through this process of iteration and constant learning, also using simulators like CST-Studio, it is possible to obtain a high-quality radiating device that meets the set objectives.

During this thesis work, an important result emerged: thanks to the application of acquired theoretical foundations, it was possible to develop a system capable of generating high-power electric fields (HIRF) and maintaining a wide frequency spectrum (broadband), despite the use of high frequencies (HF). This result is of significant value, as generating high-power electric fields at high frequencies is a technically challenging task.

Within the thesis, numerous results obtained through the initial designs and subsequent optimizations of the antenna were presented. The robustness of the design was clearly evident, not only in ideal conditions but also in challenging situations. This resilience was highlighted by the introduction of a block simulating a military vehicle, which did not negatively affect the behavior and performance of the antenna in question. The performance remained unchanged compared to the ideal case, which is a result that, although expected, is far from obvious. This demonstrates the effectiveness and versatility of our design, which is able to operate successfully even in realistic and complex contexts.

The achievement of these results and performances opens up interesting prospects and could foresee the actual realization of this radiating device within CEPOLISPE, in the next phase of the SEPRON project. This possibility could constitute a significant step in transforming ideas and projects into practical and operational solutions, contributing substantially to the overall progress of the Armed Forces.

Bibliography

- [1] Marco Righero. *Descrizione del progetto SEMPROM (Smart Electronic Protection Measures)*. Tech. rep. Fondazione LINK, 2023 (cit. on p. i).
- [2] Antenna Products. *CMV-600*. URL: <https://antennas.com/wp-content/uploads/2020/06/CMV-600-Series-SpecSheet.pdf>. (accessed: 01.09.2023) (cit. on pp. iii, 46).
- [3] Alice VAGNONE Salvatore VISTATO. «Radiating Electromagnetic Systems Lecture Notes». In: Politecnico di Torino, 2020. Chap. 1, pp. 1–24 (cit. on pp. 1, 5, 6, 9).
- [4] Mario Orefice. «Notes on ELECTROMAGNETIC WAVES II Radiation from e.m. sources and antennas». In: Politecnico di Torino, 2012. Chap. 1, pp. 14–17 (cit. on pp. 5, 7).
- [5] Arpa. *Campi elettromagnetici*. URL: <https://www.arpae.it/it/temi-ambientali/campi-elettromagnetici/scopri-di-piu/cosa-sono-i-campi-elettromagnetici>. (accessed: 18.07.2023) (cit. on p. 11).
- [6] Khan Academy. *Light: Electromagnetic waves, the electromagnetic spectrum and photons*. URL: <https://www.khanacademy.org/science/physics/light-waves/introduction-to-light-waves/a/light-and-the-electromagnetic-spectrum>. (accessed: 25.07.2023) (cit. on p. 11).
- [7] Ron Schmitt. *Electromagnetics Explained*. Newnes, 2003 (cit. on p. 12).
- [8] Bundesamt für Strahlenschutz. *What are high-frequency electromagnetic fields?* URL: <https://www.bfs.de/EN/topics/emf/hff/introduction/introduction.html>. (accessed: 18.08.2023) (cit. on p. 14).
- [9] *GUIDELINES FOR LIMITING EXPOSURE TO ELECTROMAGNETIC FIELDS (100 kHz to 300 GHz)*. HEALTH PHYS, 2020, pp. 483–524 (cit. on p. 15).
- [10] *Leggi ed altri Atti Normativi, Decreto Legislativo n. 159, Gazzetta Ufficiale, 2016-08-1* (cit. on p. 15).

BIBLIOGRAPHY

- [11] *Department of Defence interface Standard, Electromagnetic Environmental Effects Requirements for Systems, MIL-STD-464D, Departments and Agencies of the Department of Defense, 2020-12/24* (cit. on pp. 18, 19).
- [12] Colin Roy. *Maximum Exposure Levels to Radiofrequency Fields – 3kHz to 300 GHz*. ARPANSA, 2002 (cit. on p. 18).
- [13] Alberto Tibaldi. «Antenne e Propagazione». In: Politecnico di Torino, 2011. Chap. 3, pp. 146–163 (cit. on p. 26).
- [14] *CST Studio Suite - Getting Started* (cit. on p. 36).